JCI The Journal of Clinical Investigation

Heterologous prime-boost vaccination protects from EBV antigen expressing lymphomas

Julia Rühl, … , Carol S. Leung, Christian Münz

J Clin Invest. 2019. https://doi.org/10.1172/JCI125364.

Research In-Press Preview Immunology

Graphical abstract

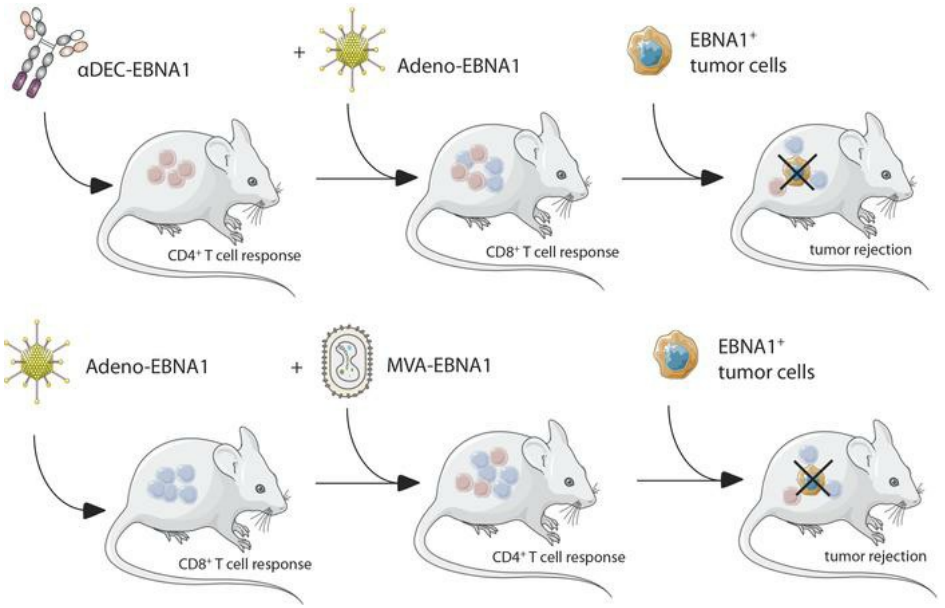

Heterologous prime-boost vaccination protects from EBV antigen expressing lymphomas

Julia Rühl[1], Carmen Citterio[1], Christine Engelmann[1], Tracey Haigh[2], Andrzej Dzionek[3], Johannes Dreyer[4], Rajiv Khanna[5], Graham S. Taylor[2], Joanna B. Wilson[6], Carol S. Leung[7,*] and Christian Münz[1,*]

[1]Viral Immunobiology, Institute of Experimental Immunology, University of Zürich, Switzerland

[2]Cancer Immunology and Immunotherapy Centre, University of Birmingham, Birmingham, UK

[3]Miltenyi Biotec GmbH, Bergisch Gladbach, Germany

[4]Institute for Pathology, Unfallkrankenhaus Berlin, Berlin, Germany

[5]QIMR Berghofer Centre for Immunotherapy and Vaccine Development and Tumour Immunology Laboratory, Department of Immunology, QIMR Berghofer Medical Research Institute, Brisbane, Australia

[6]College of Medical, Veterinary and Life Sciences, University of Glasgow, Glasgow, UK

[7]University of Oxford, Nuffield Department of Medicine, Ludwig Institute for Cancer Research, Oxford, UK

*contributed equally and corresponding authors: Carol Leung, Ludwig Institute for Cancer Research, University of Oxford, Nuffield Department of Medicine, Old Road Campus Research Building, Roosevelt Drive, Oxford OX3 7DQ, UK, e-mail: carol.leung@ludwig.ox.ac.uk, or Christian Münz, Institute of Experimental Immunology, University of Zürich, Winterthurerstrasse 190, 8057 Zürich, Switzerland, e-mail: christian.muenz@uzh.ch

Conflict of interest: AD is an employee of Miltenyi Biotec GmbH, RK is a consultant and member of the scientific advisory board of Atara Biotherapeutics and has received a license fee payment and research funding from Atara Biotherapeutics, all other authors declare no conflict of interest.

Abstract

The Epstein Barr virus (EBV) is one of the predominant tumor viruses in humans, but so far no therapeutic or prophylactic vaccination against this transforming pathogen is available. We demonstrated that heterologous prime-boost vaccination with the nuclear antigen 1 of EBV (EBNA1) either targeted to the DEC205 receptor on dendritic cells or expressed from a recombinant modified vaccinia virus Ankara (MVA) vector improved priming of antigen-specific $CD4^+$ T-cell help. This help supported the expansion and maintenance of EBNA1 specific $CD8^+$ T cells that are most efficiently primed by recombinant adenoviruses that encode EBNA1. These combined $CD4^+$ and $CD8^+$ T-cell responses protected from EBNA1 expressing T and B cell lymphomas, including lymphoproliferations that emerge spontaneously after EBNA1 expression. In particular the heterologous EBNA1-expressing adenovirus, boosted by EBNA1-encoding MVA vaccination, demonstrated protection as prophylactic and therapeutic treatment of the respective lymphoma challenges. Therefore, we suggest that such heterologous prime-boost vaccinations should be further explored for clinical development against EBV-associated malignancies as well as symptomatic primary EBV infection.

Introduction

Epstein-Barr virus (EBV) is one of the most successful human pathogens, establishing persistent infection in more than 95% of adults (1). At the same time, this common γ-herpesvirus is also the most growth-transforming pathogen *in vitro* and associated with a variety of B-cell lymphomas and epithelial cell carcinomas *in vivo* (2). These amount to around 200'000 new cancers every year, therefore EBV constitutes an important target for therapeutic intervention (3). The viral tumorigenic potential is primarily due to the latent EBV infection programs, which express up to eight proteins and more than forty non-translated RNAs (1). Together with these non-translated RNAs, the six nuclear antigens (EBNAs) and two latent membrane proteins (LMPs) of the latency III program transform B cells *in vitro* to lymphoblastoid cell lines (LCLs), and are found in non-Hodgkin's lymphomas like post-transplant lymphoproliferative disease (PTLD), immunoblastic lymphomas and diffuse large B cell lymphomas (DLBCL) of immunocompromised patients (2). The more restricted latency II program with EBNA1, LMP1 and 2 expression, is characteristic for EBV-associated Hodgkin's lymphoma, extranodal natural killer (NK)/T cell lymphomas, nasopharyngeal carcinoma and gastric carcinoma. Finally, Burkitt's lymphomas often express only EBNA1 as the sole EBV protein. Interestingly, all these EBV latency programs are already present in healthy EBV carriers in distinct differentiation stages of infected B cells (4), and EBV seems to persist long-term in memory B cells without any viral protein expression (5). The presence of growth-transforming latent EBV expression in healthy virus carriers and the increased incidence of B-cell lymphomas of all EBV latency programs in patients with primary immunodeficiencies or immune suppressive human immunodeficiency virus (HIV) co-infection (6, 7) suggest that asymptomatic persistent EBV infection relies on a comprehensive immune control of all latency patterns.

Indeed the list of primary immunodeficiencies that predispose for EBV-associated diseases identifies cytotoxic lymphocytes as the cornerstone of this immune control (6, 8). More specifically, mutations in T-cell receptor signaling identify conventional αβ T cells and innate NKT as well as γδ T cells as components of this immune control (9, 10). Among these, conventional αβ T cells have been used therapeutically after expansion with LCLs or defined EBV antigens primarily for the treatment of PTLDs (11). While the antigen specificities of these clinically efficacious T-cell transfers remain often undefined, EBNA1 has at least been identified as one of the protective EBV antigens by the treatment success after adoptive transfer of T-cell populations that have been selected via cytokine production in response to this latent EBV antigen (12). Furthermore, EBNA1 is consistently recognized at least by $CD4^+$ T cells in nearly

all healthy EBV carriers (13, 14), and both EBNA1-specific $CD4^+$ and $CD8^+$ T cells are able to target EBV-transformed B cells (15-17). For the direct recognition of EBV-transformed B cells by EBNA1-specific $CD4^+$ T cells, it has been demonstrated that this antigen is intracellularly processed for MHC class II presentation via macroautophagy (18, 19). Finally, EBNA1 is also an attractive target, because it is the sole EBV protein that is expressed in all EBV associated malignancies and can therefore serve as a viral tumor antigen to be targeted by passive and active vaccination against EBV-associated diseases (20). Thus, we aimed to identify a potent vaccine formulation to prime EBNA1-specific $CD4^+$ and $CD8^+$ T-cell responses. Our findings suggest that heterologous prime-boost vaccinations for $CD4^+$ T cell priming by either recombinant antibodies that target EBNA1 to dendritic cells using DEC205 (αDEC-E1), or modified vaccinia virus Ankara encoding EBNA1 (MVA-E1) need to be combined with $CD8^+$ T cell priming by EBNA1 encoding adenovirus (Adeno-E1&LMP) to establish efficient long-term immune control of EBNA1-expressing lymphomas. This immune control relied on both $CD4^+$ and $CD8^+$ T cell populations, which reached the highest cytotoxic $CD8^+$ T-cell frequencies and maintained a broad repertoire of $CD8^+$ T-cell effector functions only in the presence of $CD4^+$ T-cell help. We propose that our most successful prime-boost regimens (αDEC-E1 plus Adeno-E1&LMP or Adeno-E1&LMP plus MVA-IiE1) should be further developed for clinical application.

Results

Human CD4$^+$ and CD8$^+$ T-cell recognition of EBNA1 carrying or encoding vaccine formulations

It has been previously demonstrated that targeting antigens to the type I transmembrane multilectin receptor DEC205 that is preferentially expressed on conventional type I DCs (cDC1s) leads to prominent CD4$^+$ T-cell responses but has only a subtle effect on CD8$^+$ T-cell induction *in vitro* and *in vivo* (21-24). To potentially identify a more suitable receptor for enhanced antigen delivery to both MHC class I and II pathways, we constructed fusion proteins of EBNA1 and antibodies directed at nine other receptors with different internalization kinetics and expressed by similar or different myeloid cell subsets (as indicated in brackets): BDCA3 (cDC1s), CD206 (monocytes), CD207 (DCs), CD209 (Langerhans cells and cDC1s), CD40 (all antigen presenting cells), HLA-DR (all antigen presenting cells), CD1c (cDC2s) and CD11c (in blood primarily DCs).

In the first step towards the generation of EBNA1-Ab (antibody) fusion proteins the variable region sequences of the chosen antibodies were selected from mouse hybridoma cell lines. The sequenced variable regions of the heavy and light chains were synthesized into HEK expression vectors and the sequence coding for EBNA1 amino acids 400-641 was added to the heavy chain vector.

The EBNA1-Ab fusion proteins that were produced consisted of human constant regions including kappa light chain and IgG1 heavy chain, the EBNA1$_{400-641}$ sequence and a His-tag for easier detection and purification (Figure 1a). The fusion antibodies only differ in their variable regions. EBNA1-Ab fusion proteins were produced in stable infected HEK293T cell lines and their purification was monitored by SDS-PAGE and EBNA1 Western blot, with which the heavy chain can be detected at an apparent weight of around 100kD (Figure 1b, Supplemental Figure 1b). Binding specificity after cloning was confirmed through a competitive binding assay in which binding of the original hybridoma antibodies on a target cell could be overcome by prior incubation with the engineered antibody constructs (Supplemental Figure 1a). EBNA1-Ab for all eight receptors and for DEC205 were produced and maintained their receptor binding activity.

To assess the MHC class I and II presentation of these receptor-targeted EBNA1-Abs, EBNA1-specific CD4$^+$ and CD8$^+$ T-cell clones were generated from healthy EBV carriers. CD4$^+$ T-cell clones recognizing different epitopes, designated SNP restricted through HLA-DR51, NLR restricted through HLA-DR1 and AEG restricted through HLA-DQ2/3, were used. In addition, established EBNA1 specific CD8$^+$ T-cell clones were used that were specific for the HPV epitope restricted through HLA-B35, because this specificity can be readily cloned from HLA-

B35 positive EBV carriers. PBMCs were incubated with 1µM EBNA1-fusion antibodies for four hours and afterwards co-cultured with autologous T-cell clones. IFNγ secretion of $CD4^+$ and $CD8^+$ T cells was very low when co-cultured with untargeted PBMCs. An EBNA1-Ab fusion protein targeting to Langerin (CD207), which is not expressed on PBMCs, slightly induced IFNγ production, suggesting that alternative antigen uptake mechanisms may contribute to the background activation of T cells in this experimental setting. DEC205- and CD40-targeting significantly enhanced the $CD4^+$ T-cell activation to about 60% of the signal obtained from peptide-pulsed PBMCs that served as a positive control (Figure 1d). Antigen delivery through DEC205 also yielded one of the highest responses in $CD8^+$ T cells, and only BDCA3-targeting exceeded this and led to significant $CD8^+$ T-cell activation with secreted IFNγ levels of around 8% of the positive control (Figure 1e). Therefore, we identified BDCA3-targeting as the strongest receptor-targeting strategy for cross-presentation on MHC class I molecules. However, antigen targeting to BDCA3 did not significantly enhance cross-presentation in comparison to DEC205-directed antigen delivery.

In the past viral vectors have been shown to induce higher $CD8^+$ T-cell activation, therefore we complemented our panel of EBNA1-Ab fusion proteins with viral vectors encoding for EBNA1 or invariant chain EBNA1, namely modified vaccinia virus Ankara (MVA-E1 and MVA-IiE1), a lentivirus (Lenti-E1 and Lenti-IiE1) and an adenovirus 5 (Adeno-E1&LMP). PBMCs were incubated with MVAs and adenoviruses for 24 hours before co-culture with T-cell clones and with lentiviruses for 96 hours due to their slower infection kinetics. First, we checked EBNA1-specific $CD4^+$ T cell activation and found that all tested viral vectors triggered a response. Notably, the addition of the invariant chain to EBNA1 in MVA-IiE1 elicited higher IFNγ production. Moreover, we assessed the responses of another $CD4^+$ T-cell clone, specific for the AEG peptide, and detected strikingly high activation levels after co-culture with Adeno-E1&LMP-infected PBMCs, which reached around 400% of the peptide-pulsed positive control (Figure 1f). $CD8^+$ T-cell activation by Adeno-E1&LMP was as strong as the peptide-loaded positive control. Surprisingly, the MVA-IiE1 not only led to a higher $CD4^+$ but also $CD8^+$ T-cell activation, suggesting that the MHC class I presentation of EBNA1 benefits from the invariant chain fusion construct. Even after 96h of incubation, the tested lentiviruses did not induce an EBNA1-specific $CD8^+$ T-cell response (Figure 1g). Thus, adenoviral delivery of EBNA1 allowed for 10 fold higher $CD8^+$ T cell stimulation than any receptor targeting of EBNA1 and both MVA as well as adenoviruses stimulated EBNA1 specific $CD4^+$ T cells similar to receptor targeting by fusion antibodies.

EBNA1 expression in virus-infected cells was also analysed by Western blot. The infection of HEK293T cells by MVA-E1, Lenti-E1 and Lenti-IiE1 yielded high expression of EBNA1, whereas the EBNA1 signal after MVA-IiE1 and Adeno-E1&LMP infection was very low (Figure 1c). Since the constructs vary, the EBNA1 band is visible at different molecular weights. MVA-E1 carries EBNA1 without the Gly/Ala repeat and runs at around 45kD (25), MVA-IiE1 migrates more slowly (at a higher molecular weight) due to the additional invariant chain protein. Lenti-E1 carries only the most immunogenic part of EBNA1, the C-terminus from aa 400-641 with an approximate size of 30kD. Infection with Adeno-E1&LMP also leads to expression of the Gly/Ala repeat-deleted EBNA1 protein, however with additional LMP polyepitopes (26) it migrates at around 60kD. The analysis of viral-infected PBMCs showed a slightly different trend, MVA-IiE1 and MVA-E1 led to strong EBNA1 expression, whereas even after 96 hours of infection Lenti-IiE1 only yielded a low EBNA1 expression (Supplemental Figure 1c and d). The lower molecular weight bands, seen after MVA-IiE1 and MVA-E1 infection of PBMCs, are possibly degraded EBNA1 protein. The high activation of T-cell clones after co-culture with Adeno-E1&LMP-infected PBMCs could not be directly correlated with high EBNA1 expression in infected cells.

Comprehensive priming of mouse CD4$^+$ and CD8$^+$ T-cell responses against EBNA1 by heterologous vaccination

To investigate the different capacities of receptor-targeting strategies and viral vector infections to induce EBNA1-specific T-cell responses, homologous and heterologous prime-boost vaccinations were developed in a human DEC205 transgenic C57BL/6 mouse model. We focused on DEC205-targeting as it elicited one of the highest CD4$^+$ and CD8$^+$ T-cell responses in our *in vitro* experiments, and because targeting to other receptors did not result in substantially improved cross-presentation of EBNA1 on MHC class I molecules for CD8$^+$ T cell stimulation. We combined DEC205 targeting of antigen with the most promising viral vectors, namely Adeno-E1&LMP and MVA-IiE1, as well as Lenti-IiE1 as lentiviral vectors have been extensively explored in viral-based therapies (reviewed by (27)). In both regimens, heterologous and homologous, boosting vaccines were injected four weeks after the priming vaccines. In comparison, Adeno-E1&LMP prime plus MVA-IiE1 boost was introduced as a vaccination approach that showed recent promise in malaria vaccination (28). CD4$^+$ and CD8$^+$ T-cell responses towards the EBNA1 antigen were analysed using intracellular cytokine staining of IFNγ after re-stimulation of splenic cells for five hours with an EBNA1 peptide library that covers

amino acids 400-641 (Figure 2a, Supplemental Figure 2a). The highest $CD4^+$ T-cell response was induced by the homologous immunization with αDEC-E1 and polyIC as adjuvant (Figure 2b). Adeno-E1&LMP, Lenti-IiE1 and MVA-IiE1 only elicited mild or no $CD4^+$ T-cell responses *in vivo,* which improved significantly when these viral vectors were preceded by αDEC-E1. Increase in the frequency of IFNγ-secreting $CD4^+$ T cells was also observed after heterologous prime-boost with Adeno-E1&LMP and MVA-IiE1 in comparison to both vectors alone. However, the effect of vaccine combinations on the $CD8^+$ T-cell compartment was much more striking. A strong and significant increase in $CD8^+$ T-cell responses was seen after vaccination with αDEC-E1 followed by adenoviral or lentiviral vectors, with only Lenti-IiE1 being able to prime EBNA1-specific $CD8^+$ T cells on its own. MVA-IiE1 alone or in combination with receptor-targeting did not induce IFNγ-secreting $CD8^+$ T cells, whose proportion however was significantly enhanced after priming with Adeno-E1&LMP (Figure 2b). Hence, it can be concluded that heterologous prime-boost vaccinations increase the amount of EBNA1-specific $CD8^+$ T-cell responses in huDEC205tg mice in comparison to homologous prime-boost vaccines. Of note, using IFNγ ELISPOT and re-stimulation of splenic cells after vaccination with all single peptides of the EBNA1 peptide mix, we could show that the EBNA1-specific T-cell responses are distributed quite evenly over the whole length of the EBNA1 protein with stronger peptide recognition in four clusters (Supplemental Figure 2b). Beside IFNγ, also other Th1 cytokines like TNFα and IL-2 have been shown to play a role in anti-viral and/or anti-tumor immunity (29, 30). To assess the amount of polyfunctional EBNA1-specific T cells after different vaccination schemes, we analysed their cytokine expression profile by intracellular cytokine staining (ICS). $CD4^+$ T cells showed in general a more pronounced polyfunctional phenotype than $CD8^+$ T cells. DEC205-targeting led to the highest percentage of $CD4^+$ T cells that produced either two or three of the above-mentioned cytokines irrespective of the vaccination strategy (Figure 2c). Viral vectors induced a high amount of $CD4^+$ T cells that produced IFNγ, TNFα or IL-2 alone (Supplemental Figure 2c). Generally, $CD8^+$ T cells followed the same trend. After Adeno-E1&LMP vaccination polyfunctionality could be observed, which was slightly decreased after combination with αDEC-E1 priming. Also αDEC-E1+MVA-IiE1 vaccination led to polyfunctional $CD8^+$ T-cell responses, which was not observed by homologous MVA-IiE1 vaccination alone. Interestingly, MVA-IiE1 vaccination led to the highest amount of IL-2-secreting $CD8^+$ T cells independent of combination with αDEC-E1 or Adeno-E1&LMP. Most successful vaccines do not only induce robust T-cell responses, but also functional antibody responses. Therefore, we investigated whether the different homologous and heterologous vaccination schemes lead to αEBNA1 IgG antibody titers in the serum of vaccinated animals. In line with the strong and diverse $CD4^+$ T-cell

responses, homologous prime-boost regimen with αDEC-E1 led to the highest αEBNA1 IgG antibody titers (Figure 2d). Only Lenti-IiE1 of the investigated viral vectors led to high αEBNA1 IgG antibody titers, which correlate with the $CD4^+$ T-cell responses that are induced by Lenti-IiE1. As soon as αDEC-E1 was applied as a priming vaccine, αEBNA1 IgG antibody titers were also found elevated with the other viral vectors, Adeno-E1&LMP and MVA-IiE1. Surprisingly, the combination of Adeno-E1&LMP and MVA-IiE1 also induced good antibody responses towards EBNA1. However, these antibody responses against the nuclear EBNA1 antigen probably do not contribute to protection, but indicate the magnitude of the corresponding $CD4^+$ T-cell responses. These studies indicated that αDEC-E1 plus Adeno-E1&LMP1, αDEC-E1 plus Lenti-IiE1 and Adeno-E1&LMP plus MVA-IiE1 elicit the highest balanced $CD4^+$ and $CD8^+$ T-cell responses against EBNA1. Lentiviruses can possibly cause harm in the host, because of gene dysregulation that can occur after lentiviral genome insertion into the host genome. Because αDEC-E1 plus Lenti-IiE1 did not give a clear advantage in comparison to the αDEC-E1 plus Adeno-E1&LMP1 vaccination, we focused our vaccination strategies towards Adeno-E1&LMP1.

Persisting and potent EBNA1-specific $CD8^+$ T-cell responses upon comprehensive $CD4^+$ and $CD8^+$ T-cell priming by heterologous vaccination

It has been shown that $CD4^+$ T-cell help is not only needed for $CD8^+$ T-cell priming, but also for maintaining protective $CD8^+$ T-cell memory. $CD4^+$ T cells have been shown to assist in the priming of protective $CD8^+$ T-cell responses by CD40L/CD40-mediated DC maturation (31-33) and to maintain $CD8^+$ T-cell function via IL-2 and IL-21 (34, 35). Therefore, antigen-specific $CD4^+$ T-cell responses might augment priming of $CD8^+$ T cells against the same antigen. In order to investigate the effect of $CD4^+$ T-cell help by αDEC-E1 priming before vaccination with viral vectors, the heterologous prime-boost immunization schemes were inversed. In the inverse heterologous prime-boost vaccination the viral vectors Adeno-E1&LMP was used as a priming vaccine, and αDEC-E1 as a boost. Comparing standard with inverse heterologous prime-boost regimens demonstrated that priming with αDEC-E1 augments $CD8^+$ T-cell priming induced by Adeno-E1&LMP (Figure 3b). The inversion led to significantly lower EBNA1-specific $CD8^+$ T-cell responses. In contrast, $CD4^+$ T-cell responses as well as the amount of αEBNA1 IgG in the serum of vaccinated mice were not affected by the inversion (Figure 3a and c). The sole effect on $CD8^+$ T-cell responses supports our hypothesis that the $CD8^+$ T-cell priming and maintenance during our heterologous prime-boost vaccination is dependent on $CD4^+$ T-cell help.

To assess how long the vaccinated mice were capable of eliciting T-cell responses towards EBNA1, they were kept until week 21 post-boost. Peripheral blood mononuclear cells (PBMC) were collected two weeks post-boost and then approximately every month to test for re-stimulation capacity after EBNA1 peptide pulse in an ICS (Figure 3d). $CD4^+$ T-cell responses were in general low in the periphery, however most prominent after αDEC-E1 vaccination (not shown). $CD8^+$ T-cell responses peaked in week two post-boost. The heterologous prime-boost groups Adeno-E1&LMP+MVA-IiE1 and αDEC-E1+Adeno-E1&LMP induced the highest EBNA1-specific $CD8^+$ T-cell responses in the blood, with the latter remaining consistently high over 15 weeks. This long-term immunity was not seen after αDEC-E1+Lenti-IiE1, which may be partly due to the lower ability of the Lenti-IiE1 boosting vaccine to induce $CD4^+$ T-cell help (not shown). To investigate long-term EBNA1-specific immune responses in more detail, all mice were sacrificed in week 21 post-boost. Splenic cells were re-stimulated with EBNA1 peptide library and with HCMV pp65 peptide library as a negative control (Figure 3e and f). The overall $CD4^+$ as well as $CD8^+$ T-cell responses were lower than in short-term experiments, but EBNA1-specific $CD4^+$ T-cell responses were still detectable at time of sacrifice but at similar levels across all immunization groups (Figure 3e). After αDEC-E1+Adeno-E1&LMP immunization higher percentages of EBNA1-specific $CD4^+$ T cells could be detected in comparison to inverse Adeno-E1&LMP+αDEC-E1 and Adeno-E1&LMP+MVA-IiE1 vaccination. Mice in the heterologous prime-boost vaccine regimens showed slightly higher antigen-specific $CD8^+$ T-cell responses when compared to mice given viral vector vaccines alone (Figure 3f). Interestingly, even 21 weeks post-boost the deficit in EBNA1-specific $CD8^+$ T-cell responses, comparing αDEC-E1+Adeno-E1&LMP with inverse prime-boost Adeno-E1&LMP+αDEC-E1, was significant. B-cell responses towards EBNA1 were also investigated at this time point and we found significantly higher αEBNA1 antibody titers compared to non-vaccinated (PBS-treated) mice only in mice vaccinated with αDEC-E1 (Figure 3g). αDEC-E1+Adeno-E1&LMP and Adeno-E1&LMP+MVA-IiE1 regimens mostly gave similar results, except with respect to the longevity of the $CD8^+$ T-cell response. This was further increased in Adeno-E1&LMP+MVA-IiE1-vaccinated animals in comparison to αDEC-E1+Adeno-E1&LMP-vaccinated animals, with the latter giving a more diverse cytokine profile within the $CD8^+$ T-cell population. Hence, we chose αDEC-E1+Adeno-E1&LMP and Adeno-E1&LMP+MVA-IiE1 for further studies.

Protection from EBNA1-expressing EL4 lymphoma challenge by heterologous vaccination

To evaluate the therapeutic effect of the most potent heterologous prime-boost vaccinations, namely αDEC-E1+Adeno-E1&LMP and Adeno-E1&LMP+MVA-IiE1, an EBNA1^{+} model tumor was developed. EL4, a T-cell lymphoma cell line, was infected with Lenti-EBNA1-GFP. GFP-positive lymphoma cells were enriched by fluorescence-activated single cell sorting and assessed for EBNA1 expression by Western Blot and immune histochemistry (Supplemental Figure 3a and d). Untreated EL4-E1 tumors were investigated by histology and stained positive for CD4 and FoxP3. Only few tumor-infiltrating CD8^{+} T cells were detected (Supplemental Figure 3b). Mice were vaccinated with either αDEC-E1+Adeno-E1&LMP or Adeno-E1&LMP+MVA-IiE1 or homologously with αDEC-E1 or Adeno-E1&LMP as a comparison. Also one inverse prime-boost vaccination, Adeno-E1&LMP+αDEC-E1, was included to investigate the importance of the order of vaccines in prime-boost regimens. Mice were challenged with EL4-E1 tumor cells following two different schedules, namely after prophylactic or followed by therapeutic vaccination (Figure 4a). During prophylactic vaccination, two weeks after the boost mice were injected with 2x10^{5} EL4-E1 cells/mouse subcutaneously (s.c.). In the therapeutic setting, mice were challenged on day 0 and immunization followed within one to seven days. Tumor burden was analysed every second day by caliper measurement. In the challenge after prophylactic vaccination, in 11 out of 13 mice a complete EL4-E1 tumor rejection was seen in the case of αDEC-E1+Adeno-E1&LMP and Adeno-E1&LMP+MVA-IiE1 vaccination (Figure 4b). The survival rate of these mice was increased from 10 to 100% (Figure 4c). Homologous vaccinations led to a slower and decreased tumor growth, which was comparable to the tumor growth in the inverse prime-boost group. The spread of EL4-E1 tumor cells into lymph nodes (LNs) was significantly decreased only with Adeno-E1&LMP+MVA-IiE1 vaccination (Figure 4d). During therapeutic vaccination, EL4-E1 tumor growth was significantly decreased and slowed down with αDEC-E1+Adeno-E1&LMP and Adeno-E1&LMP+MVA-IiE1 treatment (Figure 4e). The survival of heterologously vaccinated animals was increased to around 75% (Figure 4f). During the therapeutic challenge no difference between standard and inverse αDEC-E1+Adeno-E1&LMP was found, which could suggest that early CD8^{+} T-cell responses are of similar importance to sustained CD8^{+} T-cell responses upon CD4^{+} T-cell help. Another hypothesis to explain this phenomenon would be that the tumor may have already primed T–cell responses and therefore priming by DEC205-targeting would be less important compared to the preventive setting. Interestingly, homologous vaccinations had only a mild effect on the tumor growth and survival in the therapeutic setting. However, the spread of EL4-E1 tumor cells during therapeutic challenge into LNs was prevented only with Adeno-E1&LMP+MVA-IiE1 vaccination (Figure 4g).

Thus, both αDEC-E1+Adeno-E1&LMP and Adeno-E1&LMP+MVA-IiE1 vaccinations performed best as prophylactic or therapeutic treatments during EL4-E1 challenge.

Dependence on CD4$^+$ and CD8$^+$ T-cell populations for protection from EL4-E1 challenge after heterologous vaccination

To understand the dependence of the αDEC-E1+Adeno-E1&LMP and Adeno-E1&LMP+MVA-IiE1 heterologous prime-boost vaccine formulations on CD4$^+$ and CD8$^+$ T-cell populations for protection from EL4-E1 challenge, either CD4$^+$ or CD8$^+$ T cells were depleted with antibodies on three consecutive days before prime and boost. Two weeks post-boost 2x10^5 EL4-E1 cells were injected s.c. and measured every second day by caliper (Figure 5a). Complete T-cell depletion was confirmed in blood on the day of prime and boost, furthermore a strong decrease in the respective T-cell populations of splenic cells was found even around 45 days after last depleting antibody injection (Supplemental Figure 3c). Notably, the T-cell depleted mice of the PBS-treated group did not show a significant difference of EL4-E1 tumor growth kinetics in comparison to non-depleted animals (Figure 5b). While comparing the survival of depleted vs. non-depleted mice, there was a trend towards early dropouts in the tumor challenged and CD4$^+$ or CD8$^+$ T-cell depleted mice without vaccination (Figure 5c). Following CD4$^+$ T-cell depletion, both heterologous vaccines lost the ability to control EL4-E1 tumor growth. To a lesser extent the loss of tumor control was also observed in the CD8$^+$ T-cell depleted vaccinated animals. Moreover, the survival of T-cell depleted vaccinated mice was drastically diminished in comparison to non-depleted vaccinated mice. Even so vaccinated and CD8$^+$ T cell-depleted mice still maintained some immune control of tumor growth (Figure 5b), their survival was also significantly reduced (Figure 5c), possibly due to immunopathology of more strongly stimulated EBNA1 specific CD4$^+$ T cells. In order to assess if CD4$^+$ T-cell help is required for comprehensive CD8$^+$ T-cell priming and maintenance, splenic cells were re-stimulated with the EBNA1 peptide library at sacrifice and CD8$^+$ T-cell responses were measured by IFNγ secretion in ICS (Figure 5d). A diminished EBNA1-specific CD8$^+$ T-cell response was observed after CD4$^+$ T-cell depletion in αDEC-E1+Adeno-E1&LMP vaccinated mice in comparison to the non-depleted group. This trend was also visible, however not significant, for Adeno-E1&LMP+MVA-IiE1 vaccination. In addition, we found abrogated αEBNA1 antibody titer in the heterologously vaccinated mice after CD4$^+$ T-cell depletion (Supplemental Figure 3e). To understand the importance of peripheral T-cell immunity for EL4-E1 metastasis, lymph nodes were taken and analysed for EBNA1 DNA content by qPCR normalized with ubiquitin C (UBC). In general, all

tested vaccinations reduced the number of mice with LN metastasis. However, this control was strongly decreased upon $CD8^+$ T-cell depletion in αDEC-E1+Adeno-E1&LMP vaccinated mice, whereas depletion of both T cell subsets in the Adeno-E1&LMP+MVA-IiE1 group led to a higher percentage of mice with LN metastasis (Figure 5e). All in all, this suggests that after heterologous prime-boost vaccination, the main EL4-E1 tumor site is controlled primarily by $CD4^+$ T-cell dependent processes, whereas the control over spreading tumor cells towards other organs mainly relies on peripheral EBNA1-specific $CD8^+$ T-cell immunity. We also analysed the amount of EBNA1 DNA in the isolated tumors after the depletion experiments and found that relapsing tumors after successful treatment with heterologous prime-boost vaccination such as αDEC-E1+Adeno-E1&LMP and Adeno-E1&LMP+MVA-IiE1 lost the EBNA1 DNA almost completely (Supplemental Figure 3f). This might occur due to the strategy of generating EL4-E1 by sorting for EBNA1-positive GFP-positive cells after lentiviral transduction, which yielded purities of around only 98%. The negative selection pressure on EBNA1-positive EL4 cells might be very high during the vaccinations with the result that the remaining 2% EBNA1-negative EL4 cells survive and relapse. These studies demonstrate dependence on both $CD4^+$ and $CD8^+$ T cells for protection from EL4-E1 tumor challenge after heterologous vaccination.

Protection from EBNA1-induced B cell lymphoma challenge by heterologous vaccination

To test the most promising heterologous prime-boost vaccinations against a tumor model that more closely resembles human EBV-associated malignancies, especially c-myc driven Burkitt's lymphoma, we used an EBNA1-induced B cell lymphoma with C57BL/6 background (36). These EBNA1-positive B lymphoma cells (BL-E1) occur spontaneously in LNs and spleens of EμEBNA1 transgenic mice (37) and show relatively low EBNA1 expression, which can be visualized by Western blot, but not by immune histochemistry (Supplemental Figure 4a). BL-E1 tumor cells overexpress the c-myc proto-oncogene as do Burkitt´s lymphomas. Tumorigenesis was identified to be unequivocally linked to EBNA1 expression and dependent not only on c-myc but also Mdm2 deregulation (36). To evaluate the protective value of the vaccinations against these EBNA1-induced B cell lymphomas, $3\text{-}5x10^6$ $CD19^+$ B cells, isolated from spleens of tumor-bearing EμEBNA1 transgenic mice, were injected i.v. 14 days post-boost. The mice were euthanized latest 45 days after tumor cell injection or when showing signs of sickness such as weight loss or reduced activity (Figure 6a). At sacrifice, DNA of spleen, blood, LNs and liver was isolated and analysed for EBNA1 DNA levels (Figure 6b). Following Adeno-

E1&LMP+MVA-IiE1 vaccination, the amount of EBNA1 DNA was lower in all analysed organs when compared to PBS-treated mice, whereas in the αDEC-E1+Adeno-E1&LMP group there were similar levels to the PBS control. By using the detection limit of EBNA1 DNA qPCR, the total tumor burden per mouse could be evaluated (Figure 6c). After Adeno-E1&LMP+MVA-IiE1 over half of the mice remained tumor-free in all of the investigated organs, whereas αDEC-E1+Adeno-E1&LMP vaccination led to only 35% of tumor-free mice. 45% of PBS-treated mice suffered from BL-E1 metastasis in three or more of the analysed organs, while none of the Adeno-E1&LMP+MVA-IiE1-treated mice had metastasis in more than two organs. The phenotype of EBNA1-induced B cell lymphomas was investigated earlier (36). In our study we could confirm that indeed proliferating cell nuclear antigen (PCNA), a proliferation marker like Ki67, and XIAP expression by immune histochemistry and EBNA1 by Western blot analysis strongly correlated with tumor pathology in the mice (Figure 6d and Supplemental Figure 4a). In vaccinated mice only $CD19^{high}$ expressing cells with a more typical lymphocyte morphology could be found, which indicates that these cells are classical B cells. Following $EBNA1^{+}$ tumor cell injection, $CD19^{dim}$ expressing cells in PBS-treated mice accumulated with PCNA and XIAP expression in comparison to αDEC-E1+Adeno-E1&LMP- and Adeno-E1&LMP+MVA-IiE1-treated mice. The XIAP expression is not unexpected since it was shown that EBNA1 tumorigenesis is dependent upon Mdm2 signaling, which promotes XIAP translation (36). Taken together, we conclude that αDEC-E1+Adeno-E1&LMP vaccination seems to lower the tumor burden upon BL-E1 injection, whereas Adeno-E1&LMP+MVA-IiE1 vaccination leads to a more effective reduction in tumor load, as indicated by the EBNA1 DNA load, spleen histology and EBNA1 specific Western blot analysis.

Characteristics of T-cell responses towards EBNA1-induced B cell lymphomas without and with protective vaccination

In order to investigate the different mechanisms of the vaccination strategies, used to restrict EBNA1-induced B cell lymphomas, T-cell populations were further analysed by FACS and histology. At sacrifice, splenic cells were re-stimulated with EBNA1 and HCMV control peptide libraries, $CD4^{+}$ and $CD8^{+}$ T-cell responses were measured by IFNγ secretion in ICS. Comparing vaccinated to PBS-treated mice, no difference in the percentage of IFNγ-secreting $CD4^{+}$ T cells could be observed (Figure 7a). However, the percentage of EBNA1-specific IFNγ-secreting $CD8^{+}$ T cells was significantly enhanced after Adeno-E1&LMP+MVA-IiE1 vaccination (Figure 7b). Curiously, αDEC-E1+Adeno-E1&LMP vaccination only led to a modest increase in EBNA1-

specific $CD8^+$ T cells. In recent studies, it was shown that mice with primary BL-E1 tumors had an imbalanced CD4/CD8 T cell ratio in the spleen, which was lower compared to mice without tumors (36). We observed a slight decrease of both $CD4^+$ and $CD8^+$ T cells in tumor-bearing spleens compared to tumor-free mice, which was most visible in PBS-treated mice (Supplemental Figure 4b). The different levels of the T-cell compartments were also depicted using CD4/CD8 T-cell ratio that showed a significant decrease of the CD4/CD8 T-cell ratio in the PBS-treated group (Figure 7c). The inability of $CD8^+$ T cells to respond to EBNA1 antigen restimulation in the αDEC-E1+Adeno-E1&LMP vaccinated group raised the question whether those T cells showed upregulation of the programmed cell death protein 1 (PD1), which is known to play a role in attenuating tumor immunity in many different types of cancers. Indeed, PD1 levels were strongly increased on splenic $CD8^+$ T cells of the PBS group of tumor-injected animals in comparison to healthy mice (Figure 7d). PD1 expression on $CD8^+$ T cells after αDEC-E1+Adeno-E1&LMP vaccination reached an intermediate level, which was significantly lower than in the tumor-bearing PBS-treated animals. Adeno-E1&LMP+MVA-IiE1-vaccinated animals showed a very low PD1 expression in their splenic $CD8^+$ T-cell compartment, which was independent of tumor injection. In order to examine the distribution of T cells in the affected organs, spleen sections were stained with H&E, αCD4 and αCD8 antibody (Figure 7e). While most mice that were both PBS-treated and tumor-challenged showed disruption of the white pulp and T-cell zones, αDEC-E1+Adeno-E1&LMP vaccination could attenuate this phenotype leading to small T-cell zones and differentiation of white and red pulp in some areas. In contrast, most mice of the Adeno-E1&LMP+MVA-IiE1 vaccination group had spleens with a healthy phenotype, sharp separation of red and white pulp and large T-cell zones similar to PBS-treated mice without tumor challenge. Liver sections of PBS-treated mice confirmed these alterations after BL-E1 tumor establishment, which led to high lymphocyte infiltrations and structural damage in the livers of tumor-bearing mice (Supplemental Figure 4c). Whereas αDEC-E1+Adeno-E1&LMP seems to have a similarly strong effect on EBNA1-positive T-cell lymphomas, these findings suggest that Adeno-E1&LMP+MVA-IiE1 vaccination might be much more suitable in preventing EBV-associated B cell malignancies.

Discussion

Our study identifies heterologous prime-boost regimens of preferentially $CD4^+$ and $CD8^+$ T-cell priming vaccine formulations as the superior immunization strategies to expand EBNA1-specific $CD4^+$ and $CD8^+$ T-cell responses, with Adeno/MVA being the most promising approach. These provide protection against EBV antigen expressing T- and B-cell lymphomas, the latter of which spontaneously originated from transgenic EBNA1 expression in mouse B cells and has some similarities with EBV-associated B cell lymphomas in humans, primarily latency I Burkitt's lymphomas (36, 37). Therefore, EBNA1-based heterologous prime-boost vaccinations should be further developed as therapeutic strategies against EBV-associated malignancies.

In contrast, homologous vaccinations with EBNA1-encoding recombinant viral vectors have already been attempted in patients with nasopharyngeal carcinoma (38, 39). In these studies, a recombinant MVA vector was used that encodes both EBNA1 and LMP2, and is capable of expanding specific $CD4^+$ and $CD8^+$ T cells to these two viral antigens in vitro (25). Intradermal injection of this vaccine candidate increased EBNA1- and/or LMP2-specific T-cell responses in 15 of 18 treated Chinese and in 8 of 14 British nasopharyngeal carcinoma patients (38, 39). Furthermore, this vaccination increased the proportion of T cells, specific for these two viral antigens, which produced TNFα and IFNγ and/or IL-2, suggesting their functional superiority (39). In parallel on the other side of the globe, a recombinant adenoviral vector encoding EBNA1 and HLA-A2 restricted polyepitopes of LMP1 and 2 was explored (40). In vitro stimulation with this vaccine formulation reversed the functional impairment of EBV-specific $CD8^+$ T cells of Hodgkin's lymphoma patients (26). Moreover, in vitro expansion of EBNA1- and LMP-specific T cells *in vitro* and adoptive transfer into nasopharyngeal carcinoma patients after primary tumor resection more than doubled their median overall survival (41). As in our mouse model, a balanced expansion of EBV-specific $CD4^+$ and $CD8^+$ T-cell responses was suggested to be important for these clinical effects. Previous studies in nasopharyngeal carcinoma patients showed that only transiently expanded $CD8^+$ T cells with LMP2 peptide-loaded or LMP1 as well as LMP2-encoding adenovirus infected dendritic cells led to partial clinical responses in only 2 of 16 and 1 of 12 of the patients (42-44). We explored new vaccination strategies and our findings suggest that improved $CD4^+$ and $CD8^+$ T-cell mediated EBV immune control might be achieved by heterologous prime-boost vaccinations with EBNA1 as the protective EBV antigen.

Heterologous prime-boost vaccination strategies combine different antigen delivery systems to improve the immune responses. Our *in vitro* studies compared 8 different surface receptors targeting, using EBNA1-specific $CD4^+$ and $CD8^+$ T-cell clones as the read out for the

efficiency of antigen presentation in PBMCs. DEC205 remains to be one of the most efficient targeted receptors in stimulating T cell responses (Figure 1). This is consistent with other studies using different methods in assessing the level of antigen presentation (45). However, vaccination by antigen-targeting to the dendritic cell receptor DEC205 elicits, with the exception of hen egg derived model antigens, mostly $CD4^+$ T-cell responses *in vivo* (21, 22, 46-54). This $CD4^+$ T-cell bias also led to an only modest efficacy after DEC205-targeted NY-ESO1 vaccination with tumor regression in only 2 of 45 patients (55). These $CD4^+$ T-cell responses could however be complemented with $CD8^+$ T-cell responses by a heterologous poxvirus-based vaccination for HIV gag p24 in nonhuman primates (56). Taking this study further, our studies compared the boosting of three different viral vectors after priming with DEC205, we showed that priming with DEC205 targeting and boosting with either adenoviral or lentiviral vector vaccines resulted in robust antigen-specific $CD8^+$ T-cell response, but not boosting with MVA (Figure 2 and 3). Moreover, the improved $CD4^+$ and $CD8^+$ T-cell responses by heterologous prime-boost vaccination with αDEC-E1 and Adeno-E1&LMP were translated into protection against EBV-antigen expressing lymphoma challenge.

In parallel to this development of heterologous prime-boost vaccinations with dendritic cell-targeted antigens, heterologous prime-boost vaccinations with different viral vectors were developed. Originally designed to give both $CD8^+$ T-cell mediated immune control of the liver stage and $CD4^+$ T-cell orchestrated immune suppression of the blood stage of malaria infection (57), heterologous adeno- and poxvirus vaccination was employed in clinical trials for malaria, Ebola and influenza virus antigens (28, 58-60). $CD4^+$ T-cell dependent antibody production was mainly observed after poxvirus vaccination, while adenovirus-derived antigen expression allowed for $CD8^+$ T-cell priming. This optimized $CD4^+$ and $CD8^+$ T-cell vaccination regime reduced malaria infection to one third in African adults (28) and established protection against EBV-antigen expressing T and B cell lymphomas in our study. Interestingly, αDEC-E1 plus Adeno-E1&LMP has equivalent protective efficacy in T cell lymphoma comparing to the Adeno-E1 plus MVA-IiE1 vaccination (Figure 4). Also, protein vaccines have the advantage of more readily manufactured, safe and less expensive than viral vector vaccines. The two clinical settings, in which such vaccination strategies could be tested are EBV seronegative adolescents with a 30-50% risk to develop infectious mononucleosis upon primary EBV infection (61) and patients with EBV associated lymphomas or carcinomas, the latter of which are the most frequent EBV associated malignancies with currently limited therapeutic options (3). The vaccination strategies might be less useful in patients with EBV associated lymphomas that

emerge during immune suppression, which have been successfully targeted by adoptive EBV specific T cell transfer (11). Thus, we are planning to develop the heterologous αDEC-E1 plus Adeno-E1&LMP and the heterologous Adeno-E1 plus MVA-IiE1 vaccination strategies further for improved therapeutic vaccination in EBV-associated tumor patients and prophylactic vaccination to prevent the symptomatic primary EBV infection infectious mononucleosis.

Methods

αDEC205-EBNA1 and other EBNA1-Ab fusion proteins

αDEC205-EBNA1 fusion antibodies were produced by transient transfection (calcium chloride) in human embryonic kidney (HEK) 293T cells. The fusion antibodies were tested for binding as described previously (21). All other EBNA1-Ab fusion proteins were designed and produced in collaboration with Miltenyi Biotec. Antibodies were produced in stable transfected, non-adherent HEK293T cell lines and were purified using Protein L columns (GE Healthcare) for a first purification and high performance Nickel-NTA columns (HisTrap, GE Healthcare) for a second purification step. Dialysis was performed overnight in 1l of 1xPBS with dialysis tubing from Spectral laboratories (MWCO 3.5kD). Characterization was done by SDS–polyacrylamide gel electrophoresis (PAGE) followed by Western blotting with the rat-αEBNA1 primary antibody (clone 1H4). The αEBNA1 antibody (clone 1H4) was kindly provided by Dr. Friedrich Grässer (65), and binding assays with increasing concentration of competitive pure antibodies of the same clonal specificity. For the antibody fusion proteins the following clones were used: BDCA1 (AD5-8E7), BDCA3 (AD5-14H12), CD40 (HB14), CD11c (MJ4-27G12), CD206 (DCN228), CD207 (MB22-9F5), HLA-DR (AC122), DEC205 (MG38.2).

Viral Vectors

The Adeno-E1&LMP recombinant adenoviral vector used in this study carries an EBNA1-LMP-polyepitope insert, which is incorporated into the replication-deficient mammalian vector Ad5F35 (26), as previously described (26). The modified vaccinia virus Ankara (MVA) is an attenuated vaccinia virus that has been used for smallpox vaccination (62). The MVA vector pSC11 carried a fusion protein insert of the Gly/Ala repeat-deleted EBNA1, either with Ii (MVA-IiE1) or without it (MVA-E1) (25). MVA-IiE1 and MVA-E1 viruses were produced as previously described (25). Additionally a replication-impaired lentivirus, carrying EBNA1 with and without the invariant chain (Ii) in a pHR-SIN-CSGWDNotI (pCSGW) backbone with IRES-GFP-tag was used (referred to as Lenti-E1 and Lenti-IiE1), together with the two helper plasmids pMDG and

pCMVDR8.91 (p8.9) (63). Invariant chain functions as a guiding protein for the EBNA1 protein, which targets it to the endolysosomal pathway for degradation. This facilitates processing of EBNA1 and subsequent presentation on MHC class II. To produce Lenti-E1 and Lenti-IiE1, 10^7 HEK 293T cells were transfected with the 20µg of the plasmid of interest and the two lentiviral packaging plasmids (10µg pMDG and 20µg p8.9) using transient transfection with calcium chloride. About 30-32 hours after medium exchange the virus was harvested. The viral supernatant was collected, centrifuged, filtered and purified using the Vivapure LentiSelect 40 kit (Sartorius) according to the manufacturer's protocol. The purified virus was eluted into cold PBS, aliquoted and stored at -80°C. Lenti-E1 and -IiE1 were titrated on HEK293T and were incubated for 2 days. The amount of infected cells was quantified by GFP expression using FACS Canto II. The concentration of transfection units (TU) per milliliter was calculated using (% infected cells x cells used in the titration/100 x 1000µl/µl of virus added to the well) = TU/ml.

Tumor models

EL4 cells were kindly provided by Prof. Dr. Melanie Greter (University of Zurich, Switzerland). These EL4 cells were infected by Lenti-E1 GFP, single cell sorted by FACSAria III 5L in the University of Zurich Cytometry Core Facility and reached a purity of 98% GFP^+ cells. $EBNA1^+$ B lymphoma cells were harvested as previously described (36, 37). Both cell lines were analysed for EBNA1 expression by Western Blot with rat-αEBNA1 primary antibody (clone 1H4, diluted 1:50 in PBS). The αEBNA1 antibody (clone 1H4) was kindly provided by Dr. Friedrich Grässer (64).

huDEC205tg mice

huDEC205tg C57BL/6 mice were a generous gift from Dr. Cheolho Cheong (Montreal, Canada) and were bred at 8-12 weeks of age at the local animal facility of the University of Zurich. Maintenance of the huDEC205 transgene was controlled by PCR for each mouse using the FWD primer 5'-TGGAAGAGACATGGAGAAACCT-3' and the REV primer 5'-TCTCAGGCCAGTCCAGAAGTA-3'.

T cell assays

PBMCs were obtained from whole blood of donors after red blood cell removal by density gradient centrifugation using Ficoll-Paque (GE healthcare) following the manufacturer's instructions. PBMCs were incubated either four hours with 1µg/mL of EBNA1 fusion antibodies, DMSO control or were infected with viral vectors at a MOI of 10 for 24, 48, 72 and 96 hours. As

a positive control, PBMCs were incubated with 5µM of cognate peptide for one hour. PBMCs were washed extensively with PBS and T-cell assays were performed in duplicates by co-culturing autologous EBNA1-loaded PBMCs (5 x 10^4/well) overnight with T-cell clones (5 × 10^3/well) in 96-well V-bottom plates. IFNγ released into the supernatant was measured by IFNγ ELISA (Mabtech).

αEBNA1 IgG ELISA

The αEBNA1 IgG titer was acquired from serum samples at the point of sacrifice or from plasma acquired during bleeding procedures using the EBNA IgG ELISA kit (BioRad) with goat-α-mouse-HRP conjugate diluted 1:2000 in PBS. The optical density (OD) was measured at 450nm by the TECAN microplate reader infinite M200 pro.

EBNA1 copy quantification by qPCR

DNA from single cell suspensions from blood, spleen, liver and LNs was isolated using DNA isolation kit (Qiagen). qPCR was performed using 25ng of each sample in triplicates with TaqMan Universal PCR kit from AppliedBiosystems. Probe 5'-/56-FAM/AGGAACTGC/ZEN/CCTTGCTATTCCACA/3IBkFQ/-3', primer 5'-GGAGACGACTCAATGGTGTAAG-3' and 5'-GGTGTGTTCGTATATGGAGGTAG-3' from integrated DNA technologies was used for EBNA1 qPCR. EBNA1 abundance was normalized to the UBC housekeeping gene with probe 5'-/56-FAM/CGAGCCCAG/ZEN/TGACACCATTGAGAA/3IBkFQ/-3', primer 5'-CCTCCTTGTCCTGGATCTTTG-3' and 5'-AGGTGGGATGCAGATCTTTG-3'.

Histology

Tissue was fixed using 4% formalin and then embedded in paraffin. Histology stainings were performed by Sophistolab. For immunohistochemistry, 3 µm sections were processed on a Leica BOND-MAX or Bond-III automated immunohistochemistry system. Stainings were performed with monoclonal rat anti-mCD19 (clone 60MP31), rat anti-mCD4 (clone 4SM94), rat anti-mCD8(clone 4SM15), rat anti-FoxP3 (clone EP340) and anti-PCNA (clone PC10). EBNA1 specific immunohistochemistry was performed with the 1H4 antibody as previously described (63).

***In vivo* immunization**

Mice were injected intraperitoneally with 5 µg anti-mouse DEC205 fused with EBNA1 mAb with 50 µg poly(I:C)-LMW (polyIC) (Invivogen) as adjuvant (21) or intravenously with viral vectors at different infectious units. The adenoviral vector was administered at 10^9 PFU/mouse (40), while all other viral vectors were injected at $1.5x10^7$ TU/mouse. The immunization was boosted 10 to 14 days later with the same dose of αDEC205-E1/polyIC or a viral vector. One week after boost, the mice were sacrificed and bulk splenocytes were isolated for analysis.

In vivo T-cell depletion

T-cell depletion was performed on three consecutive days before prime and boost by injections of 200µg of either αCD4 mAb (GK1.5) or αCD8 mAb (2.43) that were commercially available from BioXCell.

Statistics

One-way Anova plus Bonferroni pre-test, two-way Anova plus Tukey's multiple comparison, Kruskal-Wallis plus Dunn's post-test, Mantel-Cox or two-tailed Mann-Whitney tests were used where indicated. P values below 0.05 were considered statistically significant.

Study approval

All animal protocols were approved by the cantonal veterinary office of the canton of Zürich, Switzerland (protocols 209/2014 and 159/2017). All studies involving human samples were reviewed and approved by the cantonal ethics committee of Zürich, Switzerland (protocol KEK-StV-Nr.19/08).

Author contributions

Conceived and designed the experiments: JR, CSL, CM. Performed the experiments: JR, CC, CE. Analyzed the data: JR, CSL, CC. Contributed reagents and materials: RK, GST, JBW, AD, TH, JD. Wrote the paper: JR, CSL and CM.

Acknowledgements

This study was supported by Cancer Research Switzerland (KFS-4091-02-2017), KFSP^{MS} and KFSP^{HHLD} of the University of Zurich, the Vontobel Foundation, the Baugarten Foundation, the Sobek Foundation, the Swiss Vaccine Research Institute, the Swiss MS Society, the Swiss National Science Foundation (310030_162560 and CRSII3_160708) and Worldwide Cancer Research (AICR#11-0516 and WCR#14-1033) to CM.

References

1. Young LS, Yap LF, and Murray PG. Epstein-Barr virus: more than 50 years old and still providing surprises. *Nat Rev Cancer.* 2016;16(12):789-802.
2. Cesarman E. Gammaherpesviruses and lymphoproliferative disorders. *Annu Rev Pathol.* 2014;9:349-72.
3. Cohen JI, Fauci AS, Varmus H, and Nabel GJ. Epstein-Barr virus: an important vaccine target for cancer prevention. *Sci Transl Med.* 2011;3(107):107fs7.
4. Babcock JG, Hochberg D, and Thorley-Lawson AD. The expression pattern of Epstein-Barr virus latent genes in vivo is dependent upon the differentiation stage of the infected B cell. *Immunity.* 2000;13(4):497-506.
5. Babcock GJ, Decker LL, Volk M, and Thorley-Lawson DA. EBV persistence in memory B cells in vivo. *Immunity.* 1998;9(3):395-404.
6. Tangye SG, Palendira U, and Edwards ES. Human immunity against EBV-lessons from the clinic. *J Exp Med.* 2017;214(2):269-83.
7. Totonchy J, and Cesarman E. Does persistent HIV replication explain continued lymphoma incidence in the era of effective antiretroviral therapy? *Curr Opin Virol.* 2016;20:71-7.
8. Cohen JI. Primary Immunodeficiencies Associated with EBV Disease. *Curr Top Microbiol Immunol.* 2015;390(Pt 1):241-65.
9. Taylor GS, Long HM, Brooks JM, Rickinson AB, and Hislop AD. The immunology of Epstein-Barr virus-induced disease. *Annu Rev Immunol.* 2015;33:787-821.
10. Münz C. Epstein-Barr Virus-Specific Immune Control by Innate Lymphocytes. *Front Immunol.* 2017;8:1658.
11. McLaughlin LP, Gottschalk S, Rooney CM, and Bollard CM. EBV-Directed T Cell Therapeutics for EBV-Associated Lymphomas. *Methods Mol Biol.* 2017;1532:255-65.
12. Icheva V, Kayser S, Wolff D, Tuve S, Kyzirakos C, Bethge W, Greil J, Albert MH, Schwinger W, Nathrath M, et al. Adoptive transfer of epstein-barr virus (EBV) nuclear antigen 1-specific t cells as treatment for EBV reactivation and lymphoproliferative disorders after allogeneic stem-cell transplantation. *J Clin Oncol.* 2013;31(1):39-48.
13. Münz C, Bickham KL, Subklewe M, Tsang ML, Chahroudi A, Kurilla MG, Zhang D, O'Donnell M, and Steinman RM. Human $CD4^+$ T lymphocytes consistently respond to the latent Epstein-Barr virus nuclear antigen EBNA1. *J Exp Med.* 2000;191(10):1649-60.
14. Long HM, Haigh TA, Gudgeon NH, Leen AM, Tsang CW, Brooks J, Landais E, Houssaint E, Lee SP, Rickinson AB, et al. $CD4^+$ T-cell responses to Epstein Barr virus

(EBV) latent-cycle antigens and the recognition of EBV-transformed lymphoblastoid cell lines. *J Virol.* 2005;79(8):4896-907.

15. Paludan C, Bickham K, Nikiforow S, Tsang ML, Goodman K, Hanekom WA, Fonteneau JF, Stevanovic S, and Münz C. EBNA1 specific $CD4^+$ Th1 cells kill Burkitt's lymphoma cells. *J Immunol.* 2002;169:1593-603.
16. Nikiforow S, Bottomly K, Miller G, and Münz C. Cytolytic $CD4^+$-T-Cell Clones Reactive to EBNA1 Inhibit Epstein-Barr Virus-Induced B-Cell Proliferation. *J Virol.* 2003;77(22):12088-104.
17. Blake N, Lee S, Redchenko I, Thomas W, Steven N, Leese A, Steigerwald-Mullen P, Kurilla MG, Frappier L, and Rickinson A. Human $CD8^+$ T cell responses to EBV EBNA1: HLA class I presentation of the (Gly-Ala)-containing protein requires exogenous processing. *Immunity.* 1997;7(6):791-802.
18. Paludan C, Schmid D, Landthaler M, Vockerodt M, Kube D, Tuschl T, and Münz C. Endogenous MHC class II processing of a viral nuclear antigen after autophagy. *Science.* 2005;307(5709):593-6.
19. Leung CS, Haigh TA, Mackay LK, Rickinson AB, and Taylor GS. Nuclear location of an endogenously expressed antigen, EBNA1, restricts access to macroautophagy and the range of CD4 epitope display. *Proc Natl Acad Sci U S A.* 2010;107(5):2165-70.
20. Kutok JL, and Wang F. Spectrum of Epstein-Barr virus-associated diseases. *Annu Rev Pathol.* 2006;1:375-404.
21. Gurer C, Strowig T, Brilot F, Pack M, Trumpfheller C, Arrey F, Park CG, Steinman RM, and Münz C. Targeting the nuclear antigen 1 of Epstein Barr virus to the human endocytic receptor DEC-205 stimulates protective T-cell responses. *Blood.* 2008;112:1231-9.
22. Meixlsperger S, Leung CS, Ramer PC, Pack M, Vanoaica LD, Breton G, Pascolo S, Salazar AM, Dzionek A, Schmitz J, et al. $CD141^+$ dendritic cells produce prominent amounts of IFN-alpha after dsRNA recognition and can be targeted via DEC-205 in humanized mice. *Blood.* 2013;121(25):5034-44.
23. Leung CS, Maurer MA, Meixlsperger S, Lippmann A, Cheong C, Zuo J, Haigh TA, Taylor GS, and Münz C. Robust T-cell stimulation by Epstein-Barr virus-transformed B cells after antigen targeting to DEC-205. *Blood.* 2013;121(9):1584-94.
24. Ngu LN, Nji NN, Ambada GE, Sagnia B, Sake CN, Tchadji JC, Njambe Priso GD, Lissom A, Tchouangueu TF, Manga Tebit D, et al. In vivo targeting of protein antigens to dendritic cells using anti-DEC-205 single chain antibody improves HIV Gag specific

$CD4^+$ T cell responses protecting from airway challenge with recombinant vaccinia-gag virus. *Immun Inflamm Dis.* 2017, in press.

25. Taylor GS, Haigh TA, Gudgeon NH, Phelps RJ, Lee SP, Steven NM, and Rickinson AB. Dual stimulation of Epstein-Barr Virus (EBV)-specific $CD4^+$- and $CD8^+$-T-cell responses by a chimeric antigen construct: potential therapeutic vaccine for EBV-positive nasopharyngeal carcinoma. *J Virol.* 2004;78(2):768-78.
26. Smith C, Cooper L, Burgess M, Rist M, Webb N, Lambley E, Tellam J, Marlton P, Seymour JF, Gandhi M, et al. Functional reversion of antigen-specific $CD8^+$ T cells from patients with Hodgkin lymphoma following in vitro stimulation with recombinant polyepitope. *J Immunol.* 2006;177(7):4897-906.
27. Milone MC, and O'Doherty U. Clinical use of lentiviral vectors. *Leukemia.* 2018; 32(7):1529-1541.
28. Ogwang C, Kimani D, Edwards NJ, Roberts R, Mwacharo J, Bowyer G, Bliss C, Hodgson SH, Njuguna P, Viebig NK, et al. Prime-boost vaccination with chimpanzee adenovirus and modified vaccinia Ankara encoding TRAP provides partial protection against Plasmodium falciparum infection in Kenyan adults. *Sci Transl Med.* 2015;7(286):286re5.
29. Manusama ER, Stavast J, Durante NM, Marquet RL, and Eggermont AM. Isolated limb perfusion with TNF alpha and melphalan in a rat osteosarcoma model: a new anti-tumour approach. *Eur J Surg Oncol.* 1996;22(2):152-7.
30. Wrangle JM, Patterson A, Johnson CB, Neitzke DJ, Mehrotra S, Denlinger CE, Paulos CM, Li Z, Cole DJ, and Rubinstein MP. IL-2 and Beyond in Cancer Immunotherapy. *J Interferon Cytokine Res.* 2018;38(2):45-68.
31. Bennett SR, Carbone FR, Karamalis F, Flavell RA, Miller JF, and Heath WR. Help for cytotoxic-T-cell responses is mediated by CD40 signalling. *Nature.* 1998;393(6684):478-80.
32. Ridge JP, Di Rosa F, and Matzinger P. A conditioned dendritic cell can be a temporal bridge between a $CD4^+$ T- helper and a T-killer cell. *Nature.* 1998;393(6684):474-8.
33. Schoenberger SP, Toes RE, van der Voort EI, Offringa R, and Melief CJ. T-cell help for cytotoxic T lymphocytes is mediated by CD40-CD40L interactions. *Nature.* 1998;393(6684):480-3.
34. Frohlich A, Kisielow J, Schmitz I, Freigang S, Shamshiev AT, Weber J, Marsland BJ, Oxenius A, and Kopf M. IL-21R on T cells is critical for sustained functionality and control of chronic viral infection. *Science.* 2009;324(5934):1576-80.

35. Williams MA, Tyznik AJ, and Bevan MJ. Interleukin-2 signals during priming are required for secondary expansion of $CD8^+$ memory T cells. *Nature.* 2006;441(7095):890-3.
36. AlQarni S, Al-Sheikh Y, Campbell D, Drotar M, Hannigan A, Boyle S, Herzyk P, Kossenkov A, Armfield K, Jamieson L, et al. Lymphomas driven by Epstein-Barr virus nuclear antigen-1 (EBNA1) are dependant upon Mdm2. *Oncogene.* 2018; 37(29):3998-4012.
37. Wilson JB, Bell JL, and Levine AJ. Expression of Epstein-Barr virus nuclear antigen-1 induces B cell neoplasia in transgenic mice. *Embo J.* 1996;15(12):3117-26.
38. Hui EP, Taylor GS, Jia H, Ma BB, Chan SL, Ho R, Wong WL, Wilson S, Johnson BF, Edwards C, et al. Phase I trial of recombinant modified vaccinia ankara encoding Epstein-Barr viral tumor antigens in nasopharyngeal carcinoma patients. *Cancer Res.* 2013;73(6):1676-88.
39. Taylor GS, Jia H, Harrington K, Lee LW, Turner J, Ladell K, Price DA, Tanday M, Matthews J, Roberts C, et al. A recombinant modified vaccinia ankara vaccine encoding Epstein-Barr Virus (EBV) target antigens: a phase I trial in UK patients with EBV-positive cancer. *Clin Cancer Res.* 2014;20(19):5009-22.
40. Duraiswamy J, Bharadwaj M, Tellam J, Connolly G, Cooper L, Moss D, Thomson S, Yotnda P, and Khanna R. Induction of therapeutic T-cell responses to subdominant tumor-associated viral oncogene after immunization with replication-incompetent polyepitope adenovirus vaccine. *Cancer Res.* 2004;64(4):1483-9.
41. Smith C, Tsang J, Beagley L, Chua D, Lee V, Li V, Moss DJ, Coman W, Chan KH, Nicholls J, et al. Effective treatment of metastatic forms of Epstein-Barr virus-associated nasopharyngeal carcinoma with a novel adenovirus-based adoptive immunotherapy. *Cancer Res.* 2012;72(5):1116-25.
42. Lin CL, Lo WF, Lee TH, Ren Y, Hwang SL, Cheng YF, Chen CL, Chang YS, Lee SP, Rickinson AB, et al. Immunization with Epstein-Barr Virus (EBV) peptide-pulsed dendritic cells induces functional $CD8^+$ T-cell immunity and may lead to tumor regression in patients with EBV-positive nasopharyngeal carcinoma. *Cancer Res.* 2002;62(23):6952-8.
43. Li F, Song D, Lu Y, Zhu H, Chen Z, and He X. Delayed-type hypersensitivity (DTH) immune response related with EBV-DNA in nasopharyngeal carcinoma treated with autologous dendritic cell vaccination after radiotherapy. *J Immunother.* 2013;36(3):208-14.

44. Chia WK, Wang WW, Teo M, Tai WM, Lim WT, Tan EH, Leong SS, Sun L, Chen JJ, Gottschalk S, et al. A phase II study evaluating the safety and efficacy of an adenovirus-DeltaLMP1-LMP2 transduced dendritic cell vaccine in patients with advanced metastatic nasopharyngeal carcinoma. *Ann Oncol.* 2012;23(4):997-1005.
45. Reuter A, Panozza SE, Macri C, Dumont C, Li J, Liu H, Segura E, Vega-Ramos J, Gupta N, Caminschi I, et al. Criteria for dendritic cell receptor selection for efficient antibody-targeted vaccination. *J Immunol.* 2015;194(6):2696-705.
46. Dudziak D, Kamphorst AO, Heidkamp GF, Buchholz VR, Trumpfheller C, Yamazaki S, Cheong C, Liu K, Lee HW, Park CG, et al. Differential antigen processing by dendritic cell subsets in vivo. *Science.* 2007;315(5808):107-11.
47. Bonifaz LC, Bonnyay DP, Charalambous A, Darguste DI, Fujii S, Soares H, Brimnes MK, Moltedo B, Moran TM, and Steinman RM. In vivo targeting of antigens to maturing dendritic cells via the DEC-205 receptor improves T cell vaccination. *J Exp Med.* 2004;199(6):815-24.
48. Trumpfheller C, Finke JS, Lopez CB, Moran TM, Moltedo B, Soares H, Huang Y, Schlesinger SJ, Park CG, Nussenzweig MC, et al. Intensified and protective $CD4^+$ T cell immunity in mice with anti-dendritic cell HIV gag fusion antibody vaccine. *J Exp Med.* 2006;203(3):607-17.
49. Do Y, Koh H, Park CG, Dudziak D, Seo P, Mehandru S, Choi JH, Cheong C, Park S, Perlin DS, et al. Targeting of LcrV virulence protein from Yersinia pestis to dendritic cells protects mice against pneumonic plague. *Eur J Immunol.* 2010;40(10):2791-6.
50. Cheong C, Choi JH, Vitale L, He LZ, Trumpfheller C, Bozzacco L, Do Y, Nchinda G, Park SH, Dandamudi DB, et al. Improved cellular and humoral immune responses in vivo following targeting of HIV Gag to dendritic cells within human anti-human DEC205 monoclonal antibody. *Blood.* 2010;116(19):3828-38.
51. Tewari K, Flynn BJ, Boscardin SB, Kastenmueller K, Salazar AM, Anderson CA, Soundarapandian V, Ahumada A, Keler T, Hoffman SL, et al. Poly(I:C) is an effective adjuvant for antibody and multi-functional $CD4^+$ T cell responses to Plasmodium falciparum circumsporozoite protein (CSP) and alphaDEC-CSP in non human primates. *Vaccine.* 2010;28(45):7256-66.
52. Pantel A, Cheong C, Dandamudi D, Shrestha E, Mehandru S, Brane L, Ruane D, Teixeira A, Bozzacco L, Steinman RM, et al. A new synthetic TLR4 agonist, GLA, allows dendritic cells targeted with antigen to elicit Th1 T-cell immunity in vivo. *Eur J Immunol.* 2012;42(1):101-9.

53. Ruane D, Do Y, Brane L, Garg A, Bozzacco L, Kraus T, Caskey M, Salazar A, Trumpheller C, and Mehandru S. A dendritic cell targeted vaccine induces long-term HIV-specific immunity within the gastrointestinal tract. *Mucosal Immunol.* 2016;9(5):1340-52.
54. Lakhrif Z, Moreau A, Herault B, Di-Tommaso A, Juste M, Moire N, Dimier-Poisson I, Mevelec MN, and Aubrey N. Targeted Delivery of Toxoplasma gondii Antigens to Dendritic Cells Promote Immunogenicity and Protective Efficiency against Toxoplasmosis. *Front Immunol.* 2018;9(317.
55. Dhodapkar MV, Sznol M, Zhao B, Wang D, Carvajal RD, Keohan ML, Chuang E, Sanborn RE, Lutzky J, Powderly J, et al. Induction of antigen-specific immunity with a vaccine targeting NY-ESO-1 to the dendritic cell receptor DEC-205. *Sci Transl Med.* 2014;6(232):232ra51.
56. Flynn BJ, Kastenmuller K, Wille-Reece U, Tomaras GD, Alam M, Lindsay RW, Salazar AM, Perdiguero B, Gomez CE, Wagner R, et al. Immunization with HIV Gag targeted to dendritic cells followed by recombinant New York vaccinia virus induces robust T-cell immunity in nonhuman primates. *Proc Natl Acad Sci U S A.* 2011;108(17):7131-6.
57. Draper SJ, Goodman AL, Biswas S, Forbes EK, Moore AC, Gilbert SC, and Hill AV. Recombinant viral vaccines expressing merozoite surface protein-1 induce antibody- and T cell-mediated multistage protection against malaria. *Cell Host Microbe.* 2009;5(1):95-105.
58. Tapia MD, Sow SO, Lyke KE, Haidara FC, Diallo F, Doumbia M, Traore A, Coulibaly F, Kodio M, Onwuchekwa U, et al. Use of ChAd3-EBO-Z Ebola virus vaccine in Malian and US adults, and boosting of Malian adults with MVA-BN-Filo: a phase 1, single-blind, randomised trial, a phase 1b, open-label and double-blind, dose-escalation trial, and a nested, randomised, double-blind, placebo-controlled trial. *Lancet Infect Dis.* 2016;16(1):31-42.
59. Mensah VA, Roetynck S, Kanteh EK, Bowyer G, Ndaw A, Oko F, Bliss CM, Jagne YJ, Cortese R, Nicosia A, et al. Safety and Immunogenicity of Malaria Vectored Vaccines Given with Routine Expanded Program on Immunization Vaccines in Gambian Infants and Neonates: A Randomized Controlled Trial. *Front Immunol.* 2017;8(1551.
60. Coughlan L, Sridhar S, Payne R, Edmans M, Milicic A, Venkatraman N, Lugonja B, Clifton L, Qi C, Folegatti PM, et al. Heterologous Two-Dose Vaccination with Simian Adenovirus and Poxvirus Vectors Elicits Long-Lasting Cellular Immunity to Influenza Virus A in Healthy Adults. *EBioMedicine.* 2018;29(146-54.

61. Luzuriaga K, and Sullivan JL. Infectious mononucleosis. *N Engl J Med.* 2010;362(21):1993-2000.
62. Hill AV, Reyes-Sandoval A, O'Hara G, Ewer K, Lawrie A, Goodman A, Nicosia A, Folgori A, Colloca S, Cortese R, et al. Prime-boost vectored malaria vaccines: progress and prospects. *Hum Vaccin.* 2010;6(1):78-83.
63. Romao S, Gasser N, Becker AC, Guhl B, Bagajic M, Vanoaica LD, Ziegler U, Roesler J, Dengjel J, Reichenbach J, et al. Essential autophagy proteins stabilize pathogen containing phagosomes for prolonged MHC class II antigen processing. *J Cell Biol.* 2013;203(5):757-66.
64. Grasser FA, Murray PG, Kremmer E, Klein K, Remberger K, Feiden W, Reynolds G, Niedobitek G, Young LS, and Mueller-Lantzsch N. Monoclonal antibodies directed against the Epstein-Barr virus-encoded nuclear antigen 1 (EBNA1): immunohistologic detection of EBNA1 in the malignant cells of Hodgkin's disease. *Blood.* 1994;84(11):3792-8.

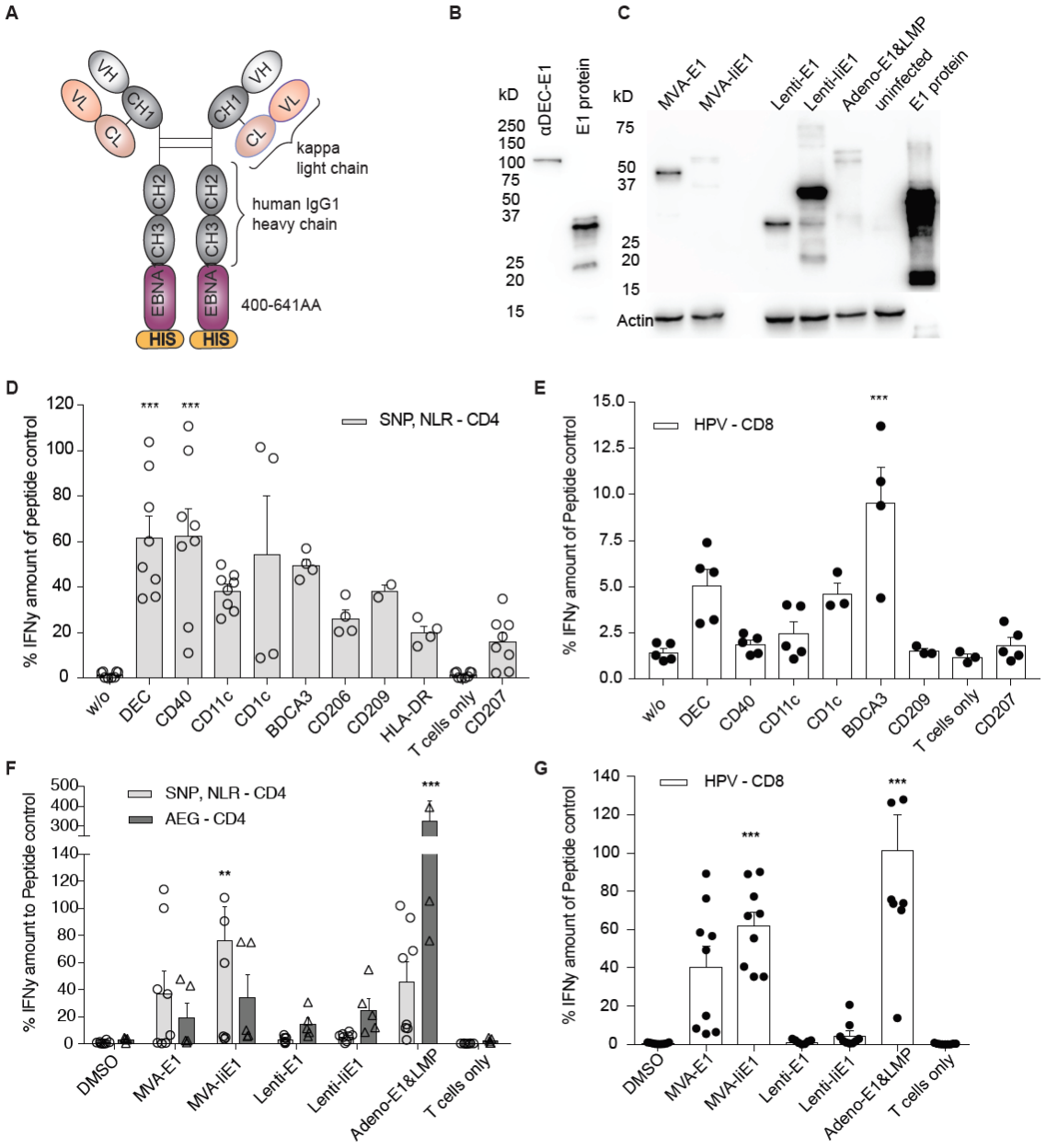

Figure 1: Human CD4⁺ and CD8⁺ T cell recognition of EBNA1 carrying or encoding vaccine formulations

A. Structure of humanized antibody-EBNA1 fusion proteins.

B. Western blot analysis of human αDEC205-EBNA1 antibody under reducing conditions using rat anti-EBNA1 Ab (clone 1H4). Lane 1 represents heavy chain - EBNA1 (100kD) and lane 2 recombinant truncated EBNA1.

C. Western blot analysis of viral vectors encoding truncated EBNA1, 48hrs after infection of HEK293T cells using rat anti-EBNA1 Ab (clone 1H4). MVA-E1 carries EBNA1 without the Gly/Ala repeat and runs at around 45kD (25), MVA-liE1 has the additional invariant chain domain. Lenti-E1 carries only EBNA1 from aa 400-641 with an approximate size of 30kD. Infection with Adeno-E1&LMP also leads to expression of the Gly/Ala repeat-deleted EBNA1 protein, however with additional LMP polyepitopes (26). It migrates at around 60kD. Lane 6 represents uninfected HEK293T cells and lane 7 recombinant truncated EBNA1.

D and E. Autologous PBMCs were incubated with medium, for 4 hours with 1 µg/mL of EBNA1 fused to an antibody against the indicated receptors or for 1 hour with the cognate peptides for the respective T-cell clones. Co-culture with (**D**) EBNA1-specific CD4⁺ T cell clones with cognate epitope NLR and SNP represented in grey bars and (**E**) EBNA1-specific CD8⁺ T cell clones with cognate epitope HPV shown in white bars. T-cell activity was measured by IFNγ release into the supernatant. IFNγ signal is given as percentage of peptide control. The mean plus SD of at least 2 independent experiments is shown. Statistical analysis was performed by one-way Anova plus Bonferroni pre-test and *P* values are represented as ****P* < .005 comparing to unspecific CD207-targeting.

F and G. Autologous PBMCs were infected with DMSO control, MVA-EBNA1, MVA-liEBNA1 or Adeno-EBNA1&LMP at a MOI of 10 for 48h and with Lenti-EBNA1 or Lenti-liEBNA1 for 96h. Co-culture with (**F**) EBNA1-specific CD4⁺ T cell clones with cognate epitope NLR and SNP with light grey bars, with cognate epitope AEG with dark grey bars and (**G**) EBNA1-specific CD8⁺ T cell clones with cognate epitope HPV with white bars. T-cell activity was determined as in D and E. Mean + SD of 2 independent experiments is shown. Statistical analysis was performed by one-way Anova plus Bonferroni pre-test and *P* values are represented as ***P* < .01 and ****P* < .005.

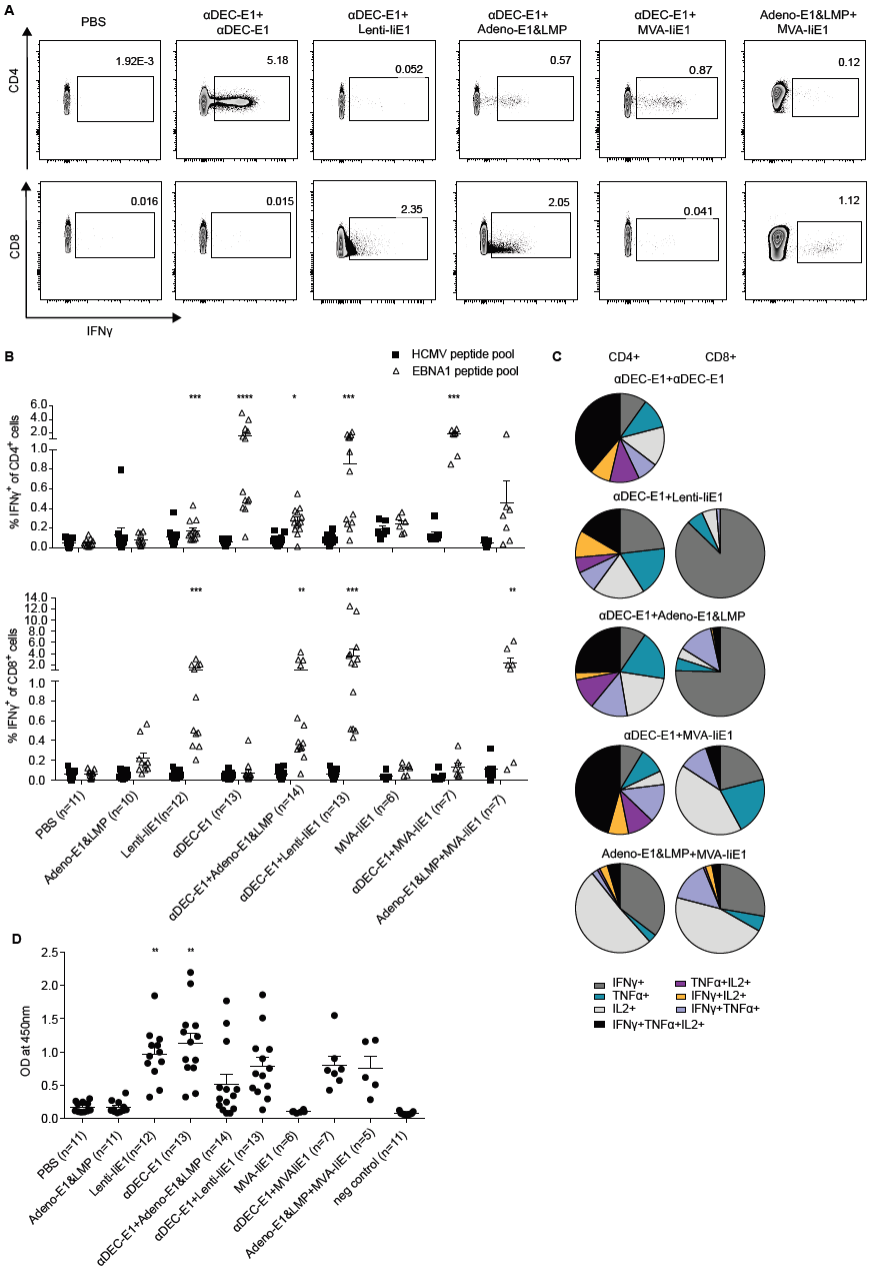

Figure 2: Comprehensive priming of mouse CD4⁺ and CD8⁺ T-cell responses against EBNA1 by heterologous vaccination in huDEC205tg mice

HuDEC205tg mice were immunized with different combinations of vaccines for prime and boost, which were set four weeks apart. Mice were sacrificed two weeks post-boost. Bulk splenocytes were harvested and stimulated either with 1 µg/mL EBNA1 or control HCMV pp65 peptide pools.

A. Representative dot plots of intracellular cytokine staining (ICS) of re-stimulated splenocytes, gated for CD4 or CD8 expression and IFNγ. One dot plot is shown for the PBS-treated and vaccination groups αDEC-E1+αDEC-E1, αDEC-E1+Lenti-IiE1, αDEC-E1+Adeno-E1&LMP, αDEC-E1+ MVA-IiE1 and Adeno-E1&LMP+MVA-IiE1 as representative examples for the data summarized in B.

B. Frequency of $CD4^+IFN\gamma^+$ and $CD8^+IFN\gamma^+$ cells from total splenocytes. Mean and SEM from four independent experiments with at least 3 mice per group are shown. Statistical analysis was done using Kruskal-Wallis test with Dunn's multiple comparison post-test. *P* values are represented as $*P < .05$, $**P < .01$ and $***P < .001$ comparing to PBS-treated mice.

C. Cytokine profile of total splenic $CD4^+$ or $CD8^+$ T cells in αDEC-E1+αDEC-E1, αDEC-E1+Lenti-IiE1, αDEC-E1+Adeno-E1&LMP, αDEC-E1+MVA-IiE1 and Adeno-E1&LMP+MVA-IiE1 vaccinated mice. Pie charts show mean of percentage of each cytokine-secreting subset.

D. Serum obtained from mice from prime-boost experiments was analysed for anti-EBNA1 IgG by ELISA. Each data point represents one individually analysed mouse. A negative control was included that contained no serum. Statistical analysis was done using Kruskal-Wallis test with Dunn's multiple comparison post-test. *P* values are represented as $*P < .05$, $**P < .01$ and $***P < .001$ comparing to PBS-treated mice. Error bars represent SEM.

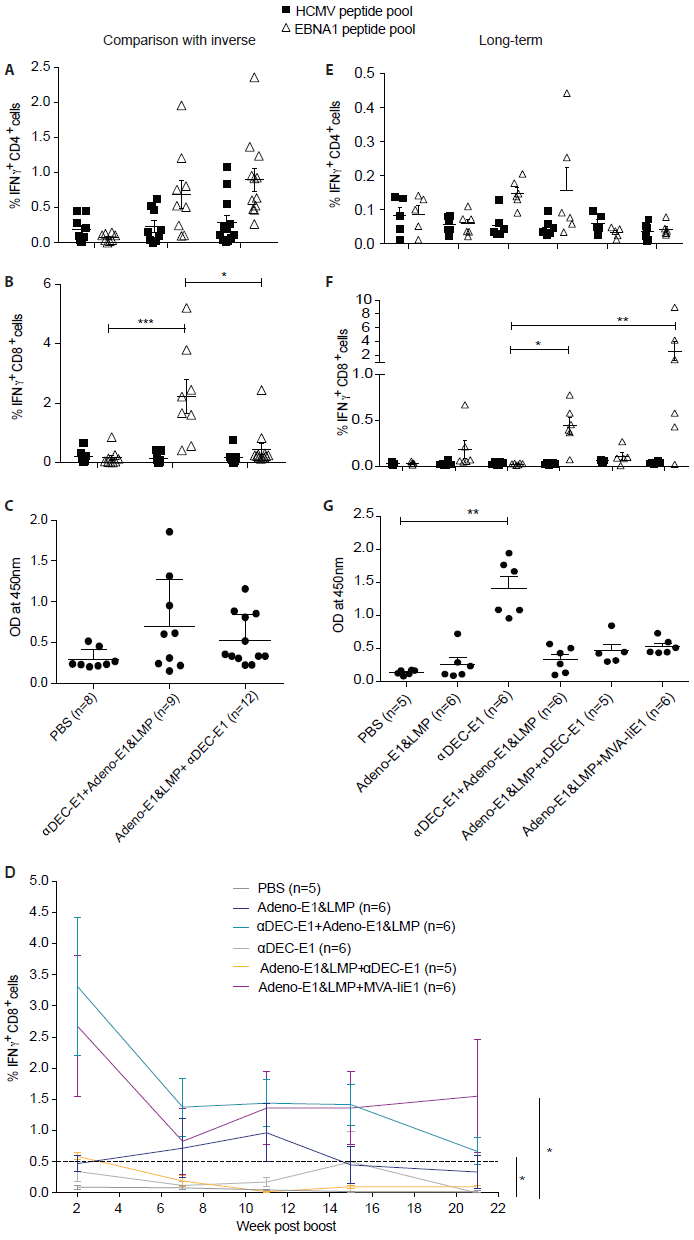

Figure 3: Persisting and potent EBNA1-specific CD8⁺ T-cell responses upon comprehensive CD4⁺ and CD8⁺ T-cell priming by heterologous vaccination

HuDEC205tg mice were immunized with different combinations of vaccines for prime and boost, which were set four weeks apart. Mice were sacrificed 2 weeks (**A-C**) or 21 weeks (**E-G**) post-boost. Bulk splenocytes were harvested and stimulated either with 1 µg/mL EBNA1 or control HCMV pp65 peptide pools. IFNγ production by CD4⁺ (**A and E**) or CD8⁺ (**B and F**) T cells was monitored by ICS. Anti-EBNA1 IgG titers were determined by ELISA (**C and G**). Each data point represents one individual mouse. Mean and SEM from three independent experiments (inverse regimen) or one long-term experiment are shown. Statistical analysis was done using Kruskal-Wallis test with Dunn's multiple comparison post-test. *P* values are represented as **P* < .05, ***P* < .01 and ****P* < .001.

D. Mice from one long-term experiment were observed up to week 21 post-boost. Blood was withdrawn in week 7, 11, 15 and 21 after the boost. PBMCs were re-stimulated with 1 µg/mL EBNA1 peptide pool after vaccination. IFNγ production was monitored by ICS in CD8⁺ cells. Mean and SEM are shown. Statistical analyses was done using two-way Anova with Tukey's multiple comparison test comparing to PBS-treated mice, *P* values are represented as **P* < .05.

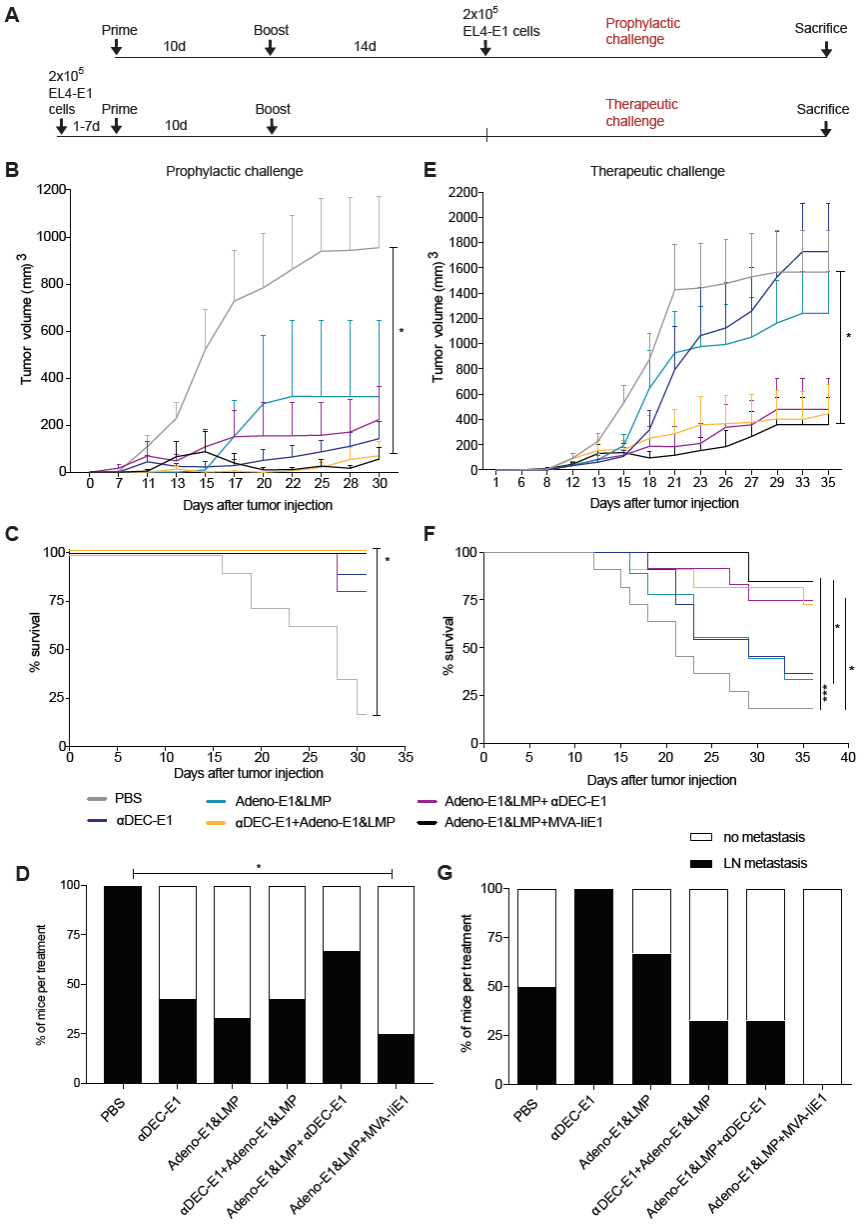

Figure 4: Protection from EBNA1-expressing EL4 lymphoma challenge by heterologous prime-boost vaccination in huDEC205tg mice.

A. HuDEC205tg mice were immunized with different combinations of vaccines for prime and boost, which were set 10 days apart. Mice were challenged with $2x10^5$ EBNA1 expressing EL4 cells (EL4-E1) s.c. either 14 days after the boost in a prophylactic setting (**B, C and D**) or one to seven days before the prime vaccination in a therapeutic setting (**E, F and G**). Mice were monitored every second day, weight was measured and tumor size was analysed by caliper. Mice were sacrificed when the tumor reached ≥15mm in diameter.

B and E. The tumor volume was calculated by the formula $A^2xBx0.52$. Mean tumor volume plus SD of three independent experiments with at least three mice per group is shown. Statistical analysis was done using two-way Anova and Tukey's multiple comparison test, *P* values represent **P* < .05 comparing to PBS-treated mice.

C and F. Percentage survival from three independent experiments with at least three mice per group is shown. Statistical analysis was done using Mantel-Cox test, *P* values represent **P* < .05 and ****P* < .001.

D and G. At sacrifice bulk single cell suspensions of lymph nodes were harvested and analysed by EBNA1 qPCR from representative prophylactic (D) and therapeutic (G) EL4-E1 tumor challenges. Abundance of EBNA1 gene is normalized to UBC gene. A tumor-load cut-off of ≥0.005 was set. The percentage of mice per condition without tumor burden and with tumor burden in the lymph nodes is depicted. Statistical analysis was done using the c_q value of the qPCR by two-way Anova and Tukey's multiple comparison test.

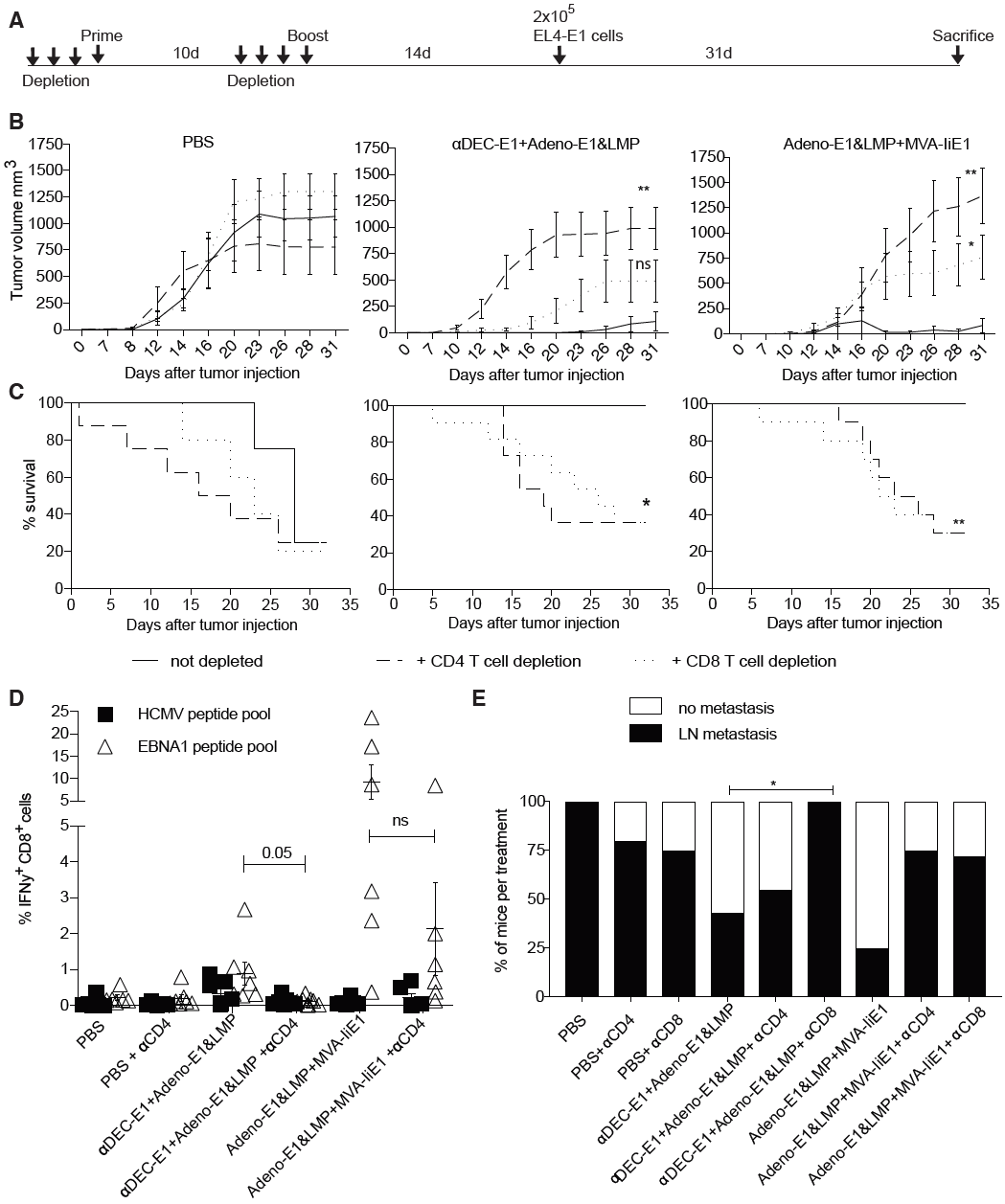

Figure 5: Dependence on CD4⁺ and CD8⁺ T-cell populations for protection from EL4-E1 challenge after heterologous vaccination

A. HuDEC205tg mice were immunized with different combinations of vaccines for prime and boost set 10 days apart. Before prime and before boost mice were depleted with injections of αCD4 or αCD8 antibody on three consecutive days. Mice were challenged with $2x10^5$ EL4-E1 cells s.c. 14 days after the boost. Mice were monitored every second day, weight was measured and tumor size was analysed by caliper.

B. Tumor growth was determined every second to third day. Tumor volume was calculated by the formula $A^2xBx0.52$. Mean tumor volume plus SD of experiment with six mice per group is shown. Statistical analysis was done by two-way Anova and Tukey's multiple comparison test, *P* values represent **P* < .05 and ***P* < .01.

C. Mice were sacrificed when the tumor reached ≥15mm in diameter. Percentage survival of one experiment with six mice per group is shown. Statistical analysis was done by Mantel-Cox test, *P* values represent **P* < .05 and ***P* < .005.

D. At the point of sacrifice bulk splenocytes were harvested and stimulated either with 1 µg/mL EBNA1 or control HCMV pp65 peptide pool. IFNγ production was monitored by ICS in $CD8^+$ gated cells. Mean and SEM from one experiment with six mice per group is shown. Statistical analysis was done using Kruskal-Wallis test with Dunn's multiple comparison post-test.

E. At sacrifice bulk single cell suspensions of lymph nodes were harvested and analysed by EBNA1 qPCR. Abundance of EBNA1 gene is normalized to UBC gene. Mean and SD from experiment with six mice per group is shown. Statistical analysis was done using the c_q value of the qPCR by two-way Anova and Tukey's multiple comparison test, *P* values represent **P* < .05.

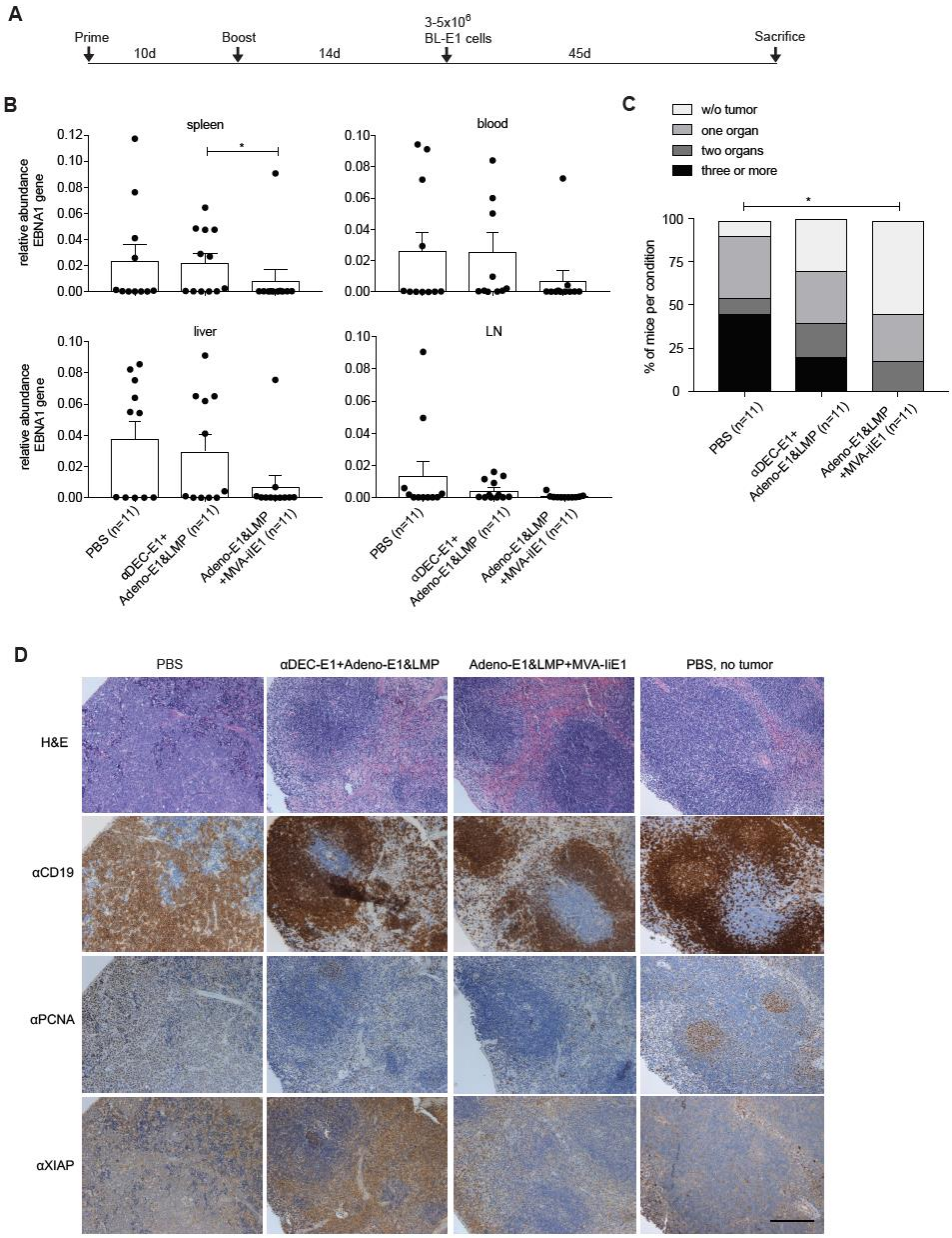

Figure 6: Protection from EBNA1-induced B-cell lymphoma challenge by heterologous vaccination

A. HuDEC205tg mice were immunized with different combinations of vaccines for prime and boost, set 10 days apart. Mice were challenged with 3-5x10^6 $EBNA1^+$ B cell tumor cells (BL-E1) i.v. 14 days after the boost in a preventive setting. Mice were monitored every second day, including weight measure and observation of general behavior and mouse grimace scale.

B. At sacrifice bulk single cell suspensions of lymph nodes, spleen, liver and blood were harvested and analysed by EBNA1 qPCR. Abundance of EBNA1 gene is normalized to UBC gene. Mean and SD from two independent experiments with at least five mice per group is shown.

C. A tumor-load cut-off of ≥0.005 was set and all analysed organs of each mouse were pooled. The percentage of mice per condition without tumor burden and with tumor burden in one to four organs is depicted. Statistical analysis was done by Mantel-Cox test, *P* values represent **P* < .05.

D. At sacrifice spleen tissues of mice with EBNA1-induced B-cell lymphoma and treatments were fixed in PFA and embedded in paraffin, as a control spleen of PBS mice without tumor treatment were used. Spleen samples were stained with H&E (upper row), αCD19 (upper middle row), αPCNA (lower middle row) and αXIAP antibodies (lower row). One representative staining for each group is shown (original magnification, scale bar 20µm).

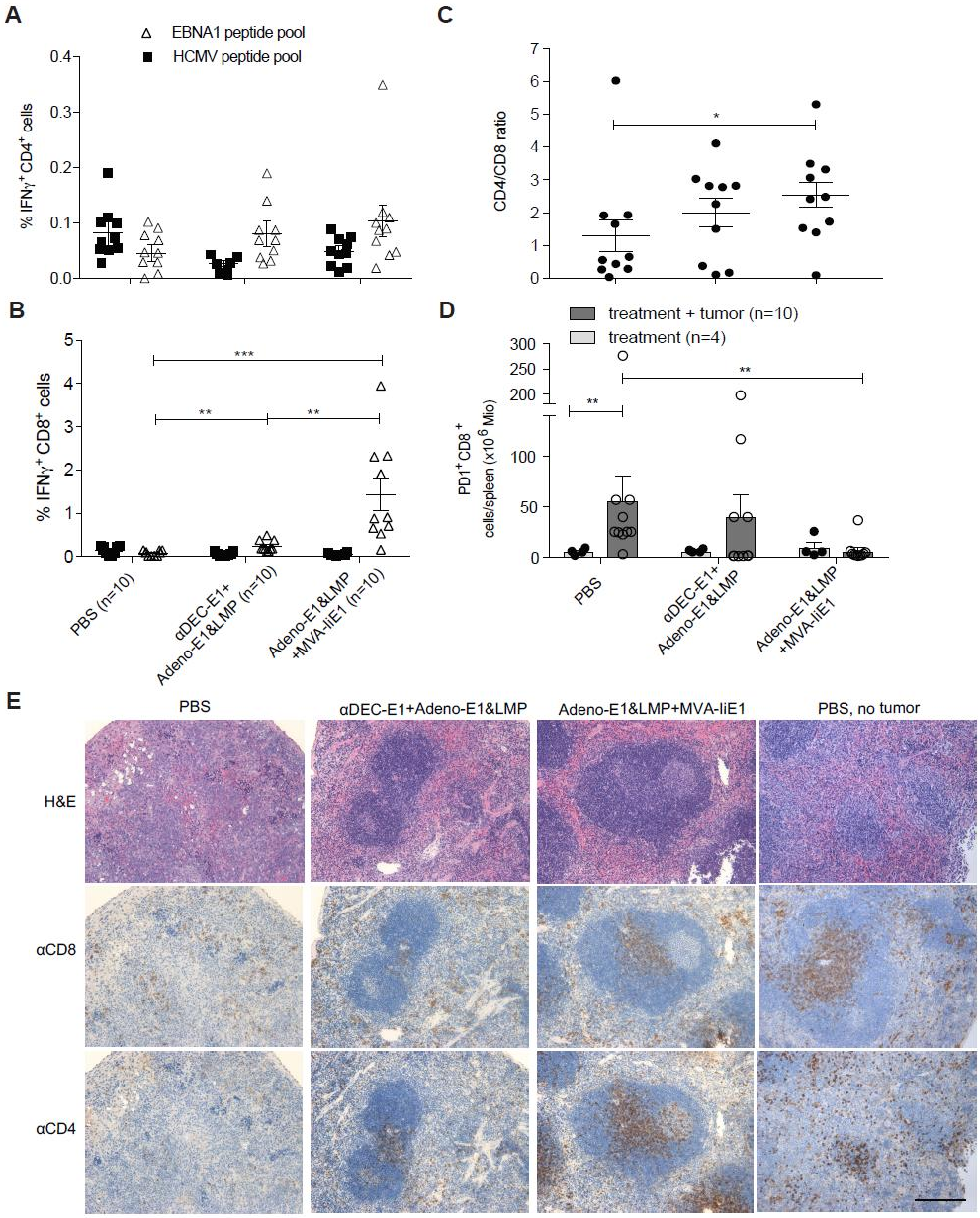

Figure 7: Characteristics of T-cell responses towards EBNA1-induced B cell lymphomas without and with protective vaccination

HuDEC205tg mice were immunized with different combinations of vaccines for prime and boost, set 10 days apart. Mice were challenged with 3-5x10^6 EBNA1$^+$ B cell tumor cells (BL-E1) i.v. 14 days after the boost in a preventive setting.

A. At sacrifice bulk splenocytes were harvested and stimulated either with 1 µg/mL EBNA1 or control HCMV pp65 peptide pools. IFNγ production was monitored by ICS in CD4$^+$ gated cells. Mean and SEM from two independent experiments with at least five mice per group are shown. Statistical analyses was done using two-tailed Mann-Whitney test.

B. After splenocyte stimulation, IFNγ production was monitored by ICS in CD8$^+$ gated cells. Mean and SEM from two independent experiments with at least five mice per group are shown. Statistical analyses was done using Kruskal-Wallis test with Dunns' multiple comparison and *P* values are represented as **P* < .05 and *****P* < .0001.

C. CD4/CD8 T cell ratio was calculated using the percentages of each subset in the spleen. Statistical analyses was done using one-way Anova with Tukey's multiple comparison test and *P* values are represented as **P* < .05 and ***P* < .005.

D. At sacrifice bulk splenocytes were harvested and stained for PD1 on CD8$^+$ gated cells. Total PD1$^+$CD8$^+$ cell amounts per spleen were calculated using the total splenocytes count. Mean and SEM from two independent experiments with at least five mice per group are shown. Mice with PBS treatment or vaccination and tumor injection are compared to mice that were only PBS-treated or vaccinated. Statistical analyses was done using Kruskal-Wallis test with Dunns' multiple comparison and *P* values are represented as **P* < .05 and ***P* < .01.

E. Spleen tissue was fixed in PFA and embedded in paraffin, stained with H&E (upper row), αCD8 (middle row) and αCD4 antibodies (lower row). One representative staining for each group is shown plus spleen staining from PBS-treated mouse without tumor challenge (original magnification, scale bar 20µm).